ADVANCED MATERIALS

Monodispersed Colloidal Spheres: Old Materials with New Applications**

By Younan Xia,* Byron Gates, Yadong Yin, and Yu Lu

This article presents an overview of current research activities that center on monodispersed colloidal spheres whose diameter falls anywhere in the range of 10 nm to 1 μm. It is organized into three parts: The first part briefly discusses several useful methods that have been developed for producing monodispersed colloidal spheres with tightly controlled sizes and well-defined properties (both surface and bulk). The second part surveys some techniques that have been demonstrated for organizing these colloidal spheres into two- and three-dimensionally ordered lattices. The third part highlights a number of unique applications of these crystalline assemblies, such as their uses as photonic bandgap (PBG) crystals; as removable templates to fabricate macroporous materials with highly ordered and three-dimensionally interconnected porous structures; as physical masks in lithographic patterning; and as diffractive elements to fabricate new types of optical sensors. Finally, we conclude with some personal perspectives on the directions towards which future research in this area might be directed.

1. Introduction

The subject of colloid science covers an extremely broad range of seemingly different systems. What these systems have in common are their constituent units: small objects that have at least one characteristic dimension in the range of 1 nm to 1 μm.[1] These objects are usually referred to as colloidal particles, and their range of size is more or less defined by the importance of Brownian motion—the endless translational diffusion of the particles resulting from the not completely averaged-out bombardment of the molecular species in the dispersion medium. In broad terms, colloidal particles can be considered as effective molecules, and be treated, to some degree, according to the theories of statistical mechanics.

Colloidal particles have long been used as the major components of industrial products such as foods, inks, paints, coatings, papers, cosmetics, photographic films, and rheological fluids.[1] They are also frequently seen and studied in materials science, chemistry, and biology. Notable examples include slurries, clays, minerals, aerosols, or foams in materials science; macromolecules (including dendrimers), aggregates of surfactant molecules, Au or Ag sols, semiconductor nanocrystallites, silica colloids, or polymer latexes in chemistry; and proteins, viruses, bacteria, or cells in biology. Figure 1 gives a partial list of these colloidal systems, together with their typical range of critical dimensions.[2] Since a number of reviews have been devoted to colloidal particles with dimensions less than 10 nm,[3–5] the scope of this article will be limited to monodispersed colloidal spheres whose diameters are in the range of 10 nm to 1 μm. The most studied and best established examples of such colloidal materials are inorganic silica colloids,[6] and polymer latexes.[7] Some of the unique aspects and niche applications of these colloidal spheres have recently been reviewed by a number of authors.[8,9] Here we intend to present an overview of the most recent activities in this area, with focus being placed on the effort that has been directed towards the fabrication of photonic bandgap (PBG) crystals and three-dimensional (3D) porous materials by employing monodispersed colloidal spheres as the building blocks.

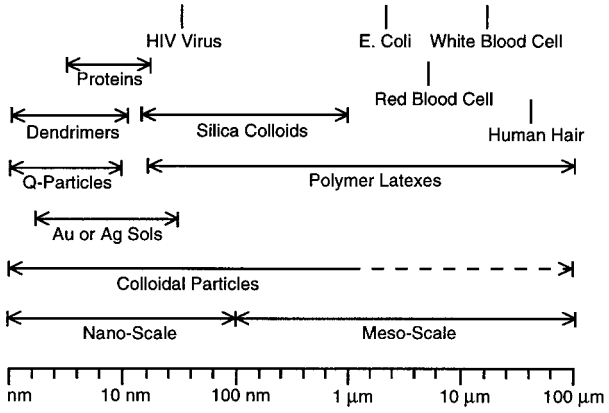

Fig. 1. A list of some representative colloidal systems, together with their typical ranges of dimensions [2]. In this chart, the upper limit of the critical dimension for colloids has been extended from 1 μm to 100 μm.

[*] Prof. Y. Xia, B. Gates
Department of Chemistry
University of Washington
Seattle, WA 98195-1700 (USA)
Y. Yin, Y. Lu
Department of Materials Science and Engineering
University of Washington
Seattle, WA 98195-2120 (USA)

[**] This work has been supported in part by a New Faculty Award from the Dreyfus Foundation, a Career Award from the National Science Foundation (DMR-9983893), a subcontract from the AFOSR MURI Center at the University of Southern California, and start-up funds from the University of Washington. B.G. thanks the Center for Nanotechnology at the UW for a fellowship.

  0935-9648/00/1005-0693 $ 17.50+.50/0

The production of monodispersed colloidal systems has been a major goal of colloid science ever since the beginning of the 20th century. Many advances in this area were brought on by the elaboration of simple, convenient, and reproducible methods that were able to generate monodispersed colloidal samples in relatively large quantities.[8] For example, the availability of colloidal particles that are uniform in size and shape plays a very important role in elucidating and understanding the electronic, optical, magnetic, and electrokinetic properties of these materials. In many cases, the employment of a monodispersed sample is also central to the self-assembly of these particles into homogeneous, crystalline arrays with large domain sizes.[9] Thanks to many years of continuous efforts, a variety of colloids can now be synthesized as truly monodispersed systems in which the size and shape of the particles and the net charges that are chemically fixed on their surfaces are all identical to within 1–2 %.[6–9] When used as stable suspensions in liquids, these colloidal particles have already found a broad range of fascinating applications in fields such as drug delivery, biodiagnostics, and combinatorial synthesis. In addition, the ability to assemble these colloidal particles into crystalline arrays allows one to obtain interesting and useful functionalities not only from the constituent materials but also from the long-range, mesoscopic order that characterizes periodic structures.[9] A natural opal, for instance, is beautifully iridescent in color because silica colloids (colorless by themselves!) have been organized into a three-dimensionally ordered array with a lattice constant that is comparable to the wavelength of visible light (400–800 nm).[10] As a result, the formation and utilization of highly ordered structures of colloidal particles has been an intriguing subject of research over the past several decades.[11]

Significant progress has been made with regard to the formation and utilization of colloidal arrays.[9] Many types of fascinating applications have also been proposed or demonstrated for this new class of materials, and some of them may have progressed past the demonstration phase. For example, 2D hexagonal lattices of colloidal spheres have been successfully demonstrated as ordered arrays of optical microlenses in image processing;[12] as physical masks for evaporation or reactive ion etching to fabricate regular arrays of micro- or nanostructures (see Sec. 7.1); and as patterned arrays of relief structures to cast elastomeric stamps for use in soft lithographic techniques.[13] On the other hand, 3D opaline lattices of colloidal spheres have recently been exploited as removable templates to generate highly ordered, macroporous materials (see Sec. 5); as diffractive elements to fabricate sensors, filters, switches, PBG crystals, or other types of optical and electrooptical devices (see Sec. 6 and 7.2); and as a directly observable (in 3D real space) model system to study a wide variety of fundamental phenomena such as crystallization, phase transition, melting, and fracture mechanics.[14] The success of all these applications strongly depends on the availability of colloidal spheres with tightly controlled sizes and surface properties, and on the ability to self-assemble them into ordered arrays with well-defined structures and sufficiently large domain sizes. It has also been shown that a tight control over the degree of perfection on the 3D periodic structure is as necessary to the photonic exploitation of crystalline arrays of colloidal spheres as has been the

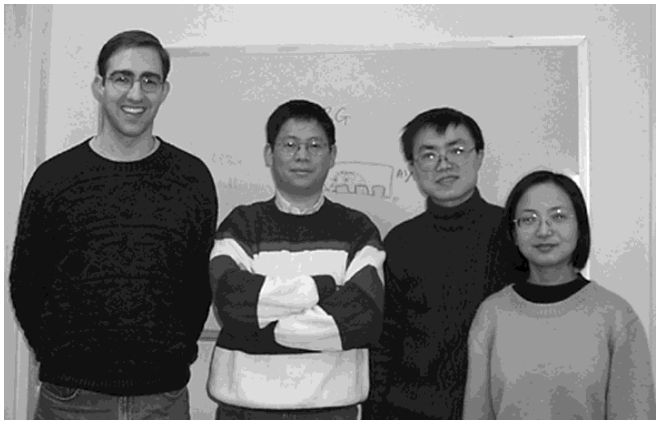

Younan Xia (second from the left) was born in Jiangsu, China, in 1965. He received a B.S. degree in chemical physics from the University of Science and Technology of China (USTC) in 1987, and then worked as a graduate student for four years at the Fujian Institute of Research on the Structure of Matter, Academia Sinica. He came to the United States in 1991, received an M.S. degree in polymer chemistry from the University of Pennsylvania (with Prof. A. G. MacDiarmid) in 1993, and a Ph.D. degree in physical chemistry from Harvard University (with Prof. G. M. Whitesides) in 1996. He has been an Assistant Professor of Chemistry at the University of Washington in Seattle since 1997. His research interests include three-dimensional microfabrication, nanostructured materials, self-assembled monolayers, inorganic functional materials, conducting polymers, microfluidic and microanalytical systems, microelectromechanical systems (MEMS), and novel devices for optics, optoelectronics, and displays. Byron Gates (first from the left) was born in Spokane, Washington (USA), in 1975. He obtained a B.S. degree in chemistry from the Western Washington University in 1997, and an M.S. degree in analytical chemistry from the University of Washington. Yadong Yin (second from the right) was born in Jiangsu, China, in 1973. He obtained his B.S. and M.S. degrees in chemistry from the USTC in 1996 and 1998, respectively. Yu Lu (first from the right) was born in Guizhou, China, in 1974. She obtained her B.S. and M.S. degrees in chemistry from the USTC in 1997 and 1999, respectively. All three are currently pursuing their Ph.D. degrees under the supervision of Prof. Y. Xia.

  0935-9648/00/1005-0694 $ 17.50+.50/0

ADVANCED MATERIALS

case in the microelectronic usage of a semiconductor. As we proceed, we will address most of these issues, which, we believe, must be addressed before colloidal arrays can reach their potential as a new class of industrial materials.

The objectives of this review are: i) to briefly discuss current approaches to the production of colloidal spheres with monodispersed sizes and desired properties; ii) to address some experimental issues related to the self-assembly of colloidal spheres into highly ordered 2D or 3D lattices; and iii) to highlight and assess a number of intriguing applications based on the intrinsic periodic structure of colloidal arrays.

2. Monodispersed Colloidal Spheres

There are a number of reasons for choosing monodispersed colloidal spheres as the primary target for scientific research. Theoretical treatments of heterogeneous systems frequently utilize the spherical symmetry. Most theoretical models (e.g., the Mie theory[15]) that deal with the properties of colloidal particles and the interactions between them are usually based on the spherical shape. In principle, the intrinsic properties of monodispersed colloidal spheres can be tightly controlled by changing the parameters illustrated in Figure 2: i) the diameter (D); ii) the chemical composition; iii) the bulk substructure; iv) the crystallinity (polycrystalline, single crystalline, or amorphous); and v) the surface functional group (thus the interfacial free energy and surface charge density). The sphere may also represent the simplest form that a colloidal particle can easily adopt during the nucleation or growth process, as driven by minimization of interfacial energy.[6–8]

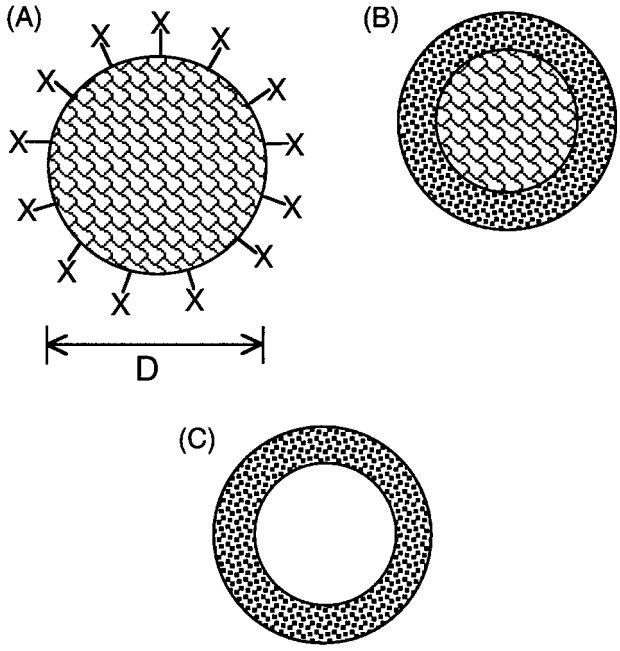

Fig. 2. Schematic illustrations of three types of representative colloidal spheres: A) a solid sphere; B) a core–shell sphere; and C) a hollow sphere. The size of the surface groups, X, has been exaggerated in (A). The polarity and density of charges on a colloidal sphere are mainly determined by the surface group. The surface of silica spheres is usually terminated in silanol groups (−Si−OH). For polymer latexes, the surface groups can span over a diverse range that includes $-NH_2$, $-COOH$, $-SO_4H$, $-SO_3H$, $-OH$, $-CONH_2$, $-CH_2NH_2$, $-CH_2Cl$, and epoxy groups. In some cases, the bulk structure (chemical composition and substructure) and surface morphology of colloidal spheres may also play an important role, although the effect of these parameters is usually neglected in most discussions.

2.1. Chemical Synthesis of Monodispersed Colloidal Spheres

A rich variety of chemical approaches are available for producing colloidal spheres that are monodispersed in size.[8] The best established and most commonly used methods seem to be controlled precipitation for inorganic (hydrous) oxides and emulsion polymerization for polymer latexes, respectively. Using these methods, inorganic oxides such as amorphous silica have been readily prepared as uniform spheres with diameter ranging from a few nm to 1 μm; polymer latexes of 20 nm to 100 μm in size have also been routinely produced as uniform beads. Figure 3 shows two transmission electron microscopy (TEM) images of such colloidal samples: ~400 nm silica spheres and ~200 nm polystyrene beads.

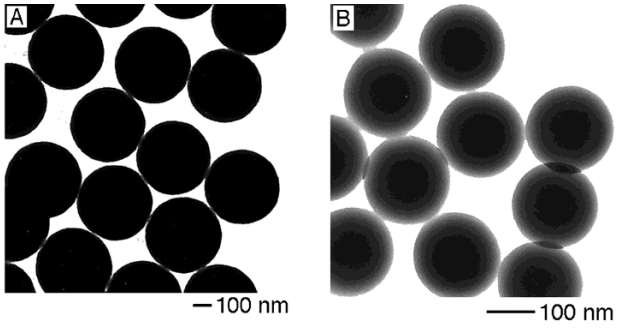

Fig. 3. The TEM images of two representative colloidal systems that can be readily prepared as monodispersed samples at large quantities: A) ~400 nm silica spheres; and B) ~200 nm polystyrene beads. Both samples were obtained from Polysciences.

2.1.1. Inorganic Colloidal Spheres by Controlled Precipitation

Inorganic colloids are usually prepared via precipitation reactions, a process that often involves two sequential steps: nucleation and growth of the nuclei. To achieve monodispersity, these two stages must be strictly separated and nucleation should be avoided during the period of growth. In a closed system, the monomer (usually exists as a complex or a solid precursor) must be added or released slowly at a well-controlled rate in order to keep it from passing the critical supersaturation levels during the growth period. This criteria for obtaining monodispersed colloidal particles was summarized by LaMer and co-workers as a general rule (the LaMer diagram) in their study of sulfur colloids prepared by acidifying thiosulfate solutions.[16] Ac-

  0935-9648/00/1005-0695 $ 17.50+.50/0

cording to this model, all the sulfur particles started at the same time and subsequently grew at the same rate until the final size was attained.

In 1968, Stöber and Fink applied this strategy to other systems and demonstrated an extremely useful procedure for preparing monodispersed silica colloids.[17] They hydrolyzed a dilute solution of tetraethylorthosilicate (TEOS) in ethanol at high pH and obtained uniform spheres of amorphous silica whose sizes could be varied from 50 nm to 2 μm simply by changing the concentrations of the reactants. This method was later improved by many others, and now seems to be the simplest and most effective route to monodispersed silica spheres.[6] Matijestic and co-workers extensively investigated and further developed this approach.[8] They have successfully applied this strategy to the production of monodispersed colloidal spheres, cubes, rods, and ellipsoids from a broad range of materials such as metal oxides and carbonates. As a general rule, it is necessary to precisely control the reaction conditions—for example, the temperature, the pH, the method for mixing of reactants, the concentration of reactants, and the concentration of counterions—to generate a single, short burst of nuclei and then let these nuclei grow uniformly.

It is worth noting that the LaMer model may not be valid for the formation of some monodispersed colloidal particles.[18] For instance, a number of recent studies suggested that several types of micrometer-sized colloidal particles prepared by the precipitation method were, in fact, the result of aggregation of much smaller subunits (or nanometer-sized primary particles) rather than continuous growth by diffusion of species from the solution towards the surfaces of nuclei.[19] In some cases, a broad range of size distribution was also observed during the period of growth, indicating the occurrence of multiple nucleation events.[20] The uniformity in size for the final product could have been achieved through a self-sharpening growth process during which small particles grew more rapidly than larger ones.

Silica colloids represent one of the best characterized inorganic systems that have been manufactured as monodispersed samples, as well as in large quantities. The surface of the as-synthesized silica colloids is often terminated with silanol groups (–Si–OH), which can ionize to generate a negatively charged interface at pH values higher than 7.[6] Pristine samples of silica colloids will undergo a series of changes when they are thermally treated at elevated temperatures: The absorbed water (~5 wt.-%) will be released first at ~150 °C; the silanol groups will be crosslinked via dehydration in the temperature range of 400–700 °C; and these particles will start to fuse into aggregates when the temperature is raised above the glass transition temperature of amorphous silica (~800 °C). The surface properties of silica colloids can be changed in a controllable way by using siloxane chemistry to form self-assembled monolayers (SAMs) with the silanol groups.[21] Other materials such as semiconductor nanocrystallites, metal sols, and organic chromophores have also been incorporated into silica colloids during the synthetic step to functionalize these particles with fluorescence or other useful optical properties.[22]

2.1.2. Polymer Latexes by Emulsion Polymerization

Polymer colloids of different chemical compositions can be produced as exceedingly uniform spheres by a process called emulsion polymerization.[7] The major components of this process include a monomer, a dispersion medium (in most cases, water), an emulsifier (surfactant), and an initiator (usually water-soluble). The monomer is dispersed as an aqueous emulsion (~1–100 μm in diameter) with the help of the emulsifier. According to the proposed mechanism, most surfactant molecules exist as micelles (~10 nm in diameter), and the majority of these micelles have been swollen by the monomer. The formation of polymer latexes begins with the decomposition of the water-soluble initiator during which a burst of primary free radicals are generated. These radicals polymerize the small amount of monomer that is dissolved in the aqueous phase to form the nuclei-oligomers in the form of tiny particles. These nuclei subsequently enter the micelles and eventually grow into larger particles until all the monomer dissolved in each micelle has been consumed. At the same time, the monomer encapsulated in emulsion droplets acts as reservoir to provide a supply of repeating units to the growing polymer chains through diffusion. The growth of polymer latexes will stop at the point when all the monomer has been depleted.[7] For a polymer latex that is 100 nm in size, there are approximately 1000 macromolecular chains entangled as coils in the sphere; each chain starts and ends with a functional group formed by the decomposition of the radical initiator.

Monodispersed polymer colloids such as poly(methyl methacrylate) (PMMA) and polystyrene (PS) have been produced in large quantities by using this technique.[7] A similar approach has also been successfully applied to the synthesis of monodispersed samples of inorganic colloidal particles.[23] The size of polymer latex spheres can be controlled at will to span a broad range from 20 nm to ~1 μm. Ugelstad et al. and El-Asser et al. developed a two-step method for preparing monodispersed polymer spheres with diameters larger than 1 μm.[24] In their approach, submicrometer-sized polystyrene beads were synthesized using the classical emulsion polymerization method, followed by swelling with another monomer (or the same monomer) in the presence of an aprotic solvent miscible with water. Subsequent polymerization of the encapsulated monomer leads to the formation of monodispersed latex spheres with diameters up to several hundred micrometers. When an immiscible monomer is introduced into the polymer beads, polymerization in the following stage may result in complex, non-spherical particles due to phase separation (see Sec. 8).

When potassium persulfate is used as the water-soluble initiator, the surface of polymer latexes prepared by emul-

  0935-9648/00/1005-0696 $ 17.50+.50/0

ADVANCED MATERIALS

sion polymerization is usually terminated in the negatively charged sulfate group.[7] Other acidic (e.g., −COOH) and basic (e.g., $-NH_2$) groups have also been introduced into the surface layer by adding the appropriate component to the monomer. The polarity of these surface groups can be changed by controlling the pH value of the dispersion medium. In some cases, both positively and negatively charged groups can also be placed on a single polymer latex particle. At a particular pH, the negative and positive charges on such latex surface are balanced and these particles are usually referred to as amphoteric or zwitterionic colloidal systems.[1]

2.2. Commercial Sources for Monodispersed Colloidal Spheres

Some monodispersed colloidal spheres can also be commercially obtained in relatively large quantities from a number of companies, although the diversity of materials might be limited. Table 1 gives a partial list (in alphabetic order) of such companies with whom we have been interacting in the past. The major products of these companies are based on silica colloids or polystyrene latexes, and are usually supplied as stabilized suspensions (>1 wt.-%) in either water or organic solvents. The polarity and density of the surface charges can be specified when orders are placed. All of these products can be directly used without further purification or separation. Several companies also take orders for customized synthesis.

It is worth noting that free samples of silica colloids can be obtained from Nissan Chemical Industries, a company that has produced silica colloids for many years and whose monodispersed products are marketed under the trade name Snowtex. In addition to its monodispersed research microspheres, Duke Scientific also provides samples that can serve as certified particle size standards. The standard deviation in diameter for these colloidal spheres is usually well-controlled in the range of 1–2 %. Dyno Particles AS seems to be the only company that provides polymer latexes with porous morphologies or core–shell structures.

2.3. Monodispersed Colloidal Spheres with Core–Shell Structures

The properties of colloidal spheres can be further modified by coating them with thin shells of a different chemical composition, as well as in varying thickness (Fig. 2B). It has been demonstrated that the structure, size, and composition of these hybrid particles could be altered in a controllable way to tailor their optical, electrical, thermal, mechanical, electro-optical, magnetic, and catalytic properties over a broad range.[25–27] This modification is also useful for tuning the interactions between colloidal spheres, and stabilizing dispersions of these spheres in a given medium. Furthermore, the cores can also be removed in a subsequent step using procedures such as solvent extraction or calcination at elevated temperatures to generate hollow spheres of the coating material

Table 1. Some commercial sources of monodispersed colloidal spheres [a].

Company	Contact Information	Size Range	General Comments
Bangs Laboratories [b]	(+1) 317 570 7020 (Tel) (+1) 317 570 7034 (Fax) info@bangslabs.com www.bangslabs.com	0.020–5.0 μm (Polystyrene) 0.3–5.0 μm (Silica)	Polystyrene (dyed, fluorescent, magnetic) and silica spheres Surface groups: carboxylic acid, aliphatic amine, chloromethyl amide, epoxy, hydrazide, aldehyde, aromatic amine, hydroxyl. Also streptavidin, secondary antibodies, Protein A, and biotin.
Duke Scientific [b]	(+1) 650 424 1177 (Tel) (+1) 650 424 1158 (Fax) info@dukesci.com www.dukesci.com	0.020–1.0 μm (Polystyrene) 0.5–1.6 μm (Silica)	Polystyrene (dyed, fluorescent) and silica spheres. Surface groups: carboxylic acid, sulfate, and a variety of others.
Dyno Particles AS	(+47) 63 89 71 00 (Tel) (+47) 63 89 74 72 (Fax) mike.griffiths@pss.aus.net www.pss.aus.net	0.5–20 μm	Polystyrene spheres (0–80% crosslinker DVB for 2–20 μm). Surface groups: carboxylic acid, amine, hydroxyl, and sulfate.
Interfacial Dynamics [b]	(+1) 503 684 8008 (Tel) (+1) 503 684 9559 (Fax) idclatex@teleport.com www.idclatex.com	0.020–10.0 μm	Polystyrene spheres (dyed, fluorescent). Surface groups: carboxylic acid, sulfate and a variety of others.
Nissan Chemicals	(+1) 713 532 4745 (Tel) (+1) 713 532 0363 (Fax) snowtex.com	0.003–0.100 μm	Colloidal silica (various dispersing media), antimony pentoxide.
Polyscience [b]	(+1) 215 343 6484 (Tel) (+1) 215 343 0214 (Fax) polysci@tigger.jvnc.net www.polysciences.com	0.05–90 μm (Polystyrene) 0.05–0.45 μm (Silica)	Polystyrene (dyed, fluorescent), silica, and glass spheres. Surface groups: carboxylic acid and sulfate.
Seradyn	(+1) 317 266 2956 (Tel) (+1) 317 266 2991 (Fax) seradyn_particles@seradyn.com ww.seradyn.com	0.05–5.0 μm	Polystyrene spheres (dyed, fluorescent, magnetic). Surface groups: carboxylic acid, streptavidin, and sulfate.

[a] Information contained here is in accordance with our knowledge of these companies at this time. [b] Custom synthesis available from these companies.

  0935-9648/00/1005-0697 $ 17.50+.50/0

(Fig. 2C).[26,28] In many cases, these hollow spheres may exhibit optical properties that are substantially different from those of solid ones. When used as fillers (or pigments), hollow spheres definitely offer advantages over their solid counterparts because hollow spheres have a much lower density. The empty interior of hollow spheres also make them particularly useful in several other niche applications. For example, they can serve as extremely small containers for encapsulation—a process that has been extensively exploited for use in catalysis, delivery of drugs, development of artificial cells, and protection of biologically active agents such as proteins, enzymes, or deoxyribonucleic acids (DNAs).[29]

A variety of methods have been successfully demonstrated for coating colloidal spheres with thin shells of the desired material. Most of them involves the use of a controlled adsorption and/or reaction (e.g., precipitation, grafted polymerization, or sol–gel condensation) on the surfaces of colloidal spheres.[30] Although these methods are straightforward to conduct, it is difficult to control the homogeneity and thickness of the coating, and sometimes this may lead to clumping and heterocoagulation. Two elegant approaches were recently demonstrated by several groups, which allowed for the generation of homogeneous, dense, thin coatings of silica on various types of colloidal spheres. In the first method, the surfaces of colloidal spheres (e.g., gold or silver colloids) were grafted with an appropriate primer that could greatly enhance the coupling (and thus deposition) of silica monomers or oligomers to these surfaces.[31] In the second method, electrostatic attractive adsorption of polyelectrolytes and charged nanoparticles was used to build a thin shell (layer-by-layer) around the template—colloidal spheres whose surfaces had been derivatized with certain charged functional groups.[32] Both methods have been successfully applied to the formation of homogeneous and dense coatings of ceramic materials on the surfaces of a variety of colloidal spheres. Subsequent removal of the core particles yielded hollow spheres made of the ceramic material.

More recently, our group also demonstrated a procedure for producing ordered arrays of mesoscale hollow spheres of ceramic materials that have a well-controlled, uniform size and homogeneous wall thickness.[33] These hollow spheres were formed by templating an appropriate sol–gel precursor against a 3D crystalline array of PS beads. Because the templating process was carried out under the confinement of two glass substrates, the thickness of the wall could be easily changed by controlling the concentration of the sol–gel precursor solution. We have demonstrated the capability and feasibility of this method by fabricating 380 and 190 nm hollow spheres of TiO_2 and SnO_2 with a wall thickness that falls anywhere in the range of 30–100 nm. Figure 4 shows the scanning electron microscopy (SEM) and TEM images of such hollow spheres that were fabricated from a sol–gel precursor to titania.[33] The thickness of the wall is approximately 50 nm.

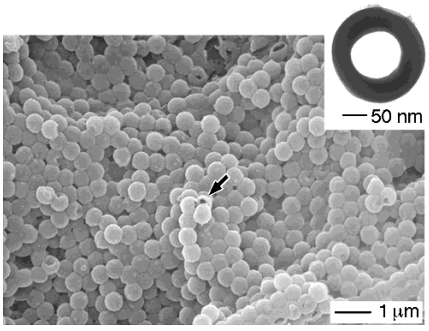

Fig. 4. An SEM image of monodispersed TiO_2 hollow spheres that were produced by templating a sol–gel precursor against a 3D crystalline array of polystyrene beads, followed by selective etching in toluene [33]. The inset shows the TEM image of such a hollow sphere, with a wall thickness of ~50 nm.

2.4. Interactions Between Colloidal Spheres Suspended in Liquids

The interactions between colloidal particles and their ramifications have been investigated intensively for almost two centuries due to their profound effect on the behavior of a colloidal dispersion, especially with respect to its stability, crystallization, and flow.[1] For hard colloidal spheres whose surfaces are electrically neutral, the pairwise potential energy of interaction consists of two terms: the short-range, steric repulsive interaction (Fig. 5A); and the

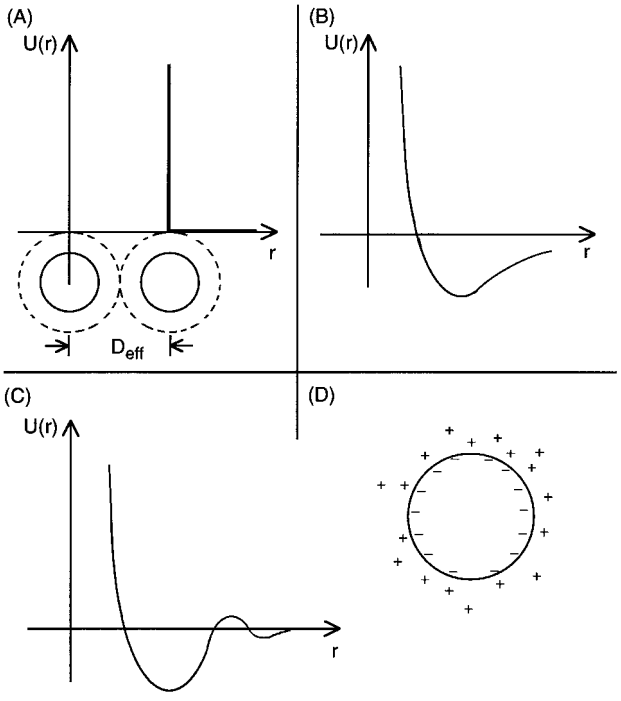

Fig. 5. A–C) The pairwise potential of interaction between two colloidal spheres: hard spheres (A); electrically neutral spheres (B); and highly charged spheres or soft spheres (C). In the ideal, hard-sphere model, there is essentially no interaction between two colloidal spheres until they approach to a distance of D_{eff}, at which the potential energy of repulsion is so strong that it effectively goes to infinity. The curve in (B) is usually referred to as the Sogami potential [1]. D) An illustration of the double-layer structure around a highly charged colloidal sphere [1].

  0935-9648/00/1005-0698 $ 17.50+.50/0

ADVANCED MATERIALS

long-range (exists over distances of ~100 nm) attractive interaction, which is usually referred to as the van der Waals (or London dispersion, or Hamaker) force. A sum of these two potential energies of interaction is plotted against the center-to-center separation in Figure 5B. For highly charged colloidal spheres suspended in a solution containing stray electrolytes, the effective pair potential is still under debate because the experiments are usually complicated by many body effects.[34,35] In general, a third term has to be added to the potential energy: that is, the much stronger, long-range Coulomb repulsion shielded by electrolytes (the so-called Yukawa potential):

$$U(r) = \frac{(Ze)^2}{\varepsilon}\left(\frac{e^{\kappa a}}{1+\kappa a}\right)^2 \frac{e^{-\kappa r}}{r} \quad (1)$$

where r is the center-to-center distance between the two spheres, Z is the number of charges per sphere, a is the radius of the sphere, and ε is the dielectric constant of the dispersion medium. The magnitude of this electrostatic repulsive force decreases strongly with increasing concentration of stray electrolytes due to the screening effect caused by the counterions present in the double layers.[36] This relationship is also characterized by the Debye–Hückel screening length $\kappa^{-1} = [4\pi(n_s Z + n_i)\lambda_B)]^{-1/2}$, a parameter that scales inversely with the square root of the ionic strength of the suspension and measures the distance over which the repulsive Coulomb potential is canceled by the screening effect of the counterions. In this equation, n_s and n_i are the concentration of spheres and counterions, and $\lambda_B = e^2/\varepsilon k_B T$ is the characteristic separation (or the Bjerrum length) between ions carrying a single electronic charge, e, at temperature T in a fluid of dielectric constant ε. The sum of these three potentials gives the well-known Derjaguin–Landau–Vervey–Overbeek (DLVO) potential,[35] which is plotted against the center-to-center separation in Figure 5C. As illustrated in Figure 5D, high levels of stray electrolytes can effectively shield the repulsive interactions between colloidal particles, and thus the van der Waals attraction prevails at all separations and the particles agglomerate. Only at very low electrolyte concentration ($<10^{-5}$ M) is the intensity of electrostatic repulsion sufficient to stabilize an ordered configuration of the particles at separations greater than a particle diameter. The interactions between charged colloidal spheres could be strongly influenced by the presence of other highly charged particles or external charged surfaces. In this case, long-range attractive interactions have also been observed among similarly charged colloidal particles, which could be explained by the redistribution of the electric double layers of ions and counterions around the particles.[37]

3. Formation of 2D Arrays of Colloidal Spheres

Monodispersed colloidal spheres can be self-assembled into ordered 2D arrays on solid supports or in thin films of liquids using a number of strategies.[38–40] Figure 6 shows the schematic diagrams of three such approaches, by which colloidal spheres have been organized into closely packed, 2D hexagonal arrays.

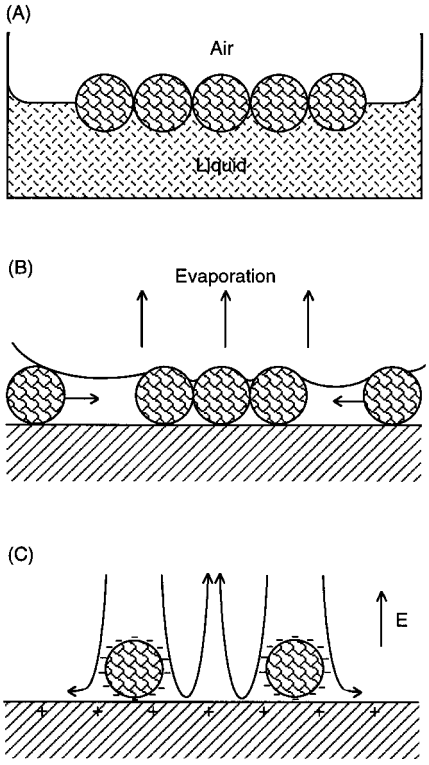

Fig. 6. Schematic illustrations of three methods that have been demonstrated for organizing monodispersed colloidal spheres into 2D hexagonal arrays: A) at the air–liquid interface via long-range attractive interactions [41]; B) in a thin liquid film spread on a solid substrate via attractive capillary forces [45]; and C) on the surface of a solid electrode via electrophoretic deposition [52].

In the first method (Fig. 6A) a 2D array of colloidal spheres is formed at the air–liquid interface; and this array can be subsequently transferred onto the surface of a solid substrate. The surfaces of these colloidal spheres have to be modified such that they will only be partially immersed into the surface of a liquid after they have been spread onto the air–liquid interface through a spreading agent (usually an alcohol).[41] It is the strong attractive interactions (e.g., those between dipoles induced by the asymmetric interface) among the colloidal spheres that lead to the spontaneous formation of a 2D aggregate at the interface. The morphology of the aggregate usually exhibits fractal characteristics; but it can also be changed by varying a number of parameters such as the size, the number concentration, the surface hydrophobicity, or the charge density on the colloids, and the electrolytic properties of the underlying liquid.[41] In a recent demonstration, for example, Kondo et al. were able to generate 2D arrays of silica colloids (1 μm in diameter) with relatively large domain sizes by controlling the degree to which the silica colloids were immersed into the liquid surface.[42] Deckman et al.,

  0935-9648/00/1005-0699 $ 17.50+.50/0

Lenzmann et al., and Fulda and Tieke applied the Langmuir–Blodgett (LB) film technique to this first method and they were able to obtain polycrystalline 2D arrays of polymer latexes over areas as large as several square centimeters.[43] More recently, Burmeister et al. also demonstrated a similar technique that was capable of forming ordered 2D arrays of colloidal spheres on various types of substrates.[44]

The second method was largely explored by Nagayama and his co-workers.[40,45] It uses the attractive capillary forces among colloidal spheres to organize them into a hexagonal 2D array in a thin film of liquid supported on a flat substrate. In a typical experiment, a liquid dispersion of colloid spheres is spread onto the surface of a solid substrate. When the solvent evaporates slowly under a controlled condition, these colloidal spheres are self-assembled into a closely packed, hexagonal array (Fig. 6B). Nagayama and co-workers also followed this self-assembly process experimentally by using an optical microscope.[40a,46] They found that a nucleus—an ordered region that consists of a number of colloidal spheres—was first formed when the thickness of the liquid layer approached the diameter of the colloids. More colloids were driven toward this nucleus by a convective transport, and eventually organized around the nucleus due to the attractive capillary forces. A flat, clean, and chemically homogeneous surface has to be used in order to generate a highly ordered array with relatively large domain sizes. Solid substrates such as glass slides or silicon wafers have been used directly in this technique. Lazarov et al. have also explored the use of liquids such as perfluorinated oil (F-oil) or mercury as the substrates in forming highly ordered 2D arrays of colloidal spheres.[47] More recently, Colvin and co-workers demonstrated the capability and feasibility of this method in forming 3D opaline lattices with well-controlled numbers of layers along the [111] direction.[48]

The evaporation of solvent can also be accelerated by carefully spin-coating a colloidal dispersion onto a solid substrate.[49] In order to obtain a uniform monolayer, it is critical that the colloidal dispersion is able to wet completely the surface of the solid substrate and there exists an electrostatic repulsion between the colloidal spheres and the solid substrate. In many cases, the wetting could be greatly improved by adding a surfactant to the colloidal dispersion or simply by precoating the substrate with a thin layer of surfactant. Van Duyne and co-workers also exploited the use of this technique to form single- and double-layered structures from colloidal spheres.[50] As observed by Deckman et al.,[49] the surfactant might form residuals on the substrate, and the domain size of the ordered region often decreases with the dimension of colloidal spheres (ordering did not occur when colloidal spheres were smaller than 50 nm). Multilayers could be obtained at relatively high solid concentrations and low spin speeds, while many defects appeared under these conditions.

The third method is usually referred to as electrophoretic deposition.[51–53] In this approach (Fig. 6C), a liquid dispersion of colloidal spheres is confined between two parallel solid electrodes such as indium tin oxide (ITO)-coated microscope coverslips. In the presence of a sufficiently strong electric field (50–100 V/cm), the colloidal spheres that have been randomly deposited on the anode will move toward each other to form a stable 2D hexagonal array. The entire process can be modulated by changing the amplitude of the applied electric field. It has been suggested that the long-range attraction between the colloidal spheres was caused by electrodynamic flows which, in turn, were induced by distortions in the applied electric field and the passage of ionic current through the solution.[52,53] This method has been applied to a number of colloidal systems, such as micrometer-sized silica colloids and polymer latexes,[52] as well as nanometer-sized gold colloids.[54] Recently, López and co-workers have also extended this method to the fabrication of 3D opaline structures from silica colloids.[55]

At the current stage of development, all of these methods are only capable of generating colloidal arrays built up by small domains, and the largest single domain usually contains fewer than 10 000 colloidal spheres.[47] These methods can also only form 2D hexagonal arrays in which the colloidal spheres are in physical contact. As a result, it is very hard to independently vary the lattice constant and the particle size. The approach based on optical forces seems to have the potential to overcome these difficulties.[56] In this method, colloidal spheres are organized into a highly ordered 2D structure in a liquid by creating an optical standing wave pattern having a regular array of intensity antinodes. The colloidal spheres are then driven to the antinode maxima by the optical forces. Depending on how many laser beams are used to create the standing wave, patterns as complex as a quasicrystal have also been produced. As demonstrated by Misawa et al. and Mio and Marr, the method based on optical forces was also capable of generating an arbitrary 2D or 3D pattern by adding individual colloidal spheres to an array one at a time.[57]

4. Fabrication of 3D Arrays of Colloidal Spheres

A rich variety of methods are available for organizing monodispersed colloidal spheres into highly ordered 3D arrays. Figure 7 shows the schematic diagrams of three representative approaches, by which colloidal spheres have been successfully assembled into 3D crystalline lattices with relatively large domain sizes.

4.1. Sedimentation in a Force Field

Sedimentation in a gravitational field (Fig. 7A) seems to be the simplest approach to the formation of 3D crystalline arrays from colloidal spheres.[1] Although it looks simple,

  0935-9648/00/1005-0700 $ 17.50+.50/0

ADVANCED MATERIALS

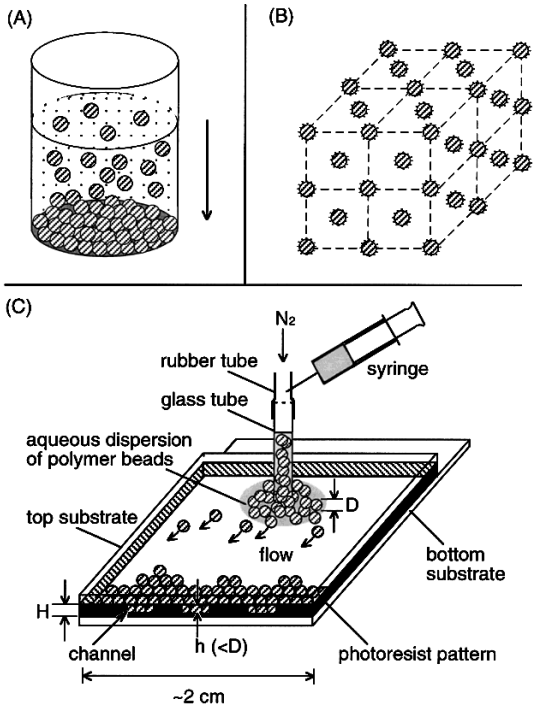

Fig. 7. Schematic outlines of three experimental procedures that have been used to assemble colloidal spheres into 3D crystalline lattices: A) sedimentation in the gravitational field [58]; B) ordering via repulsive electrostatic interactions [69]; and C) crystallization through physical confinement and hydrodynamic flow [76].

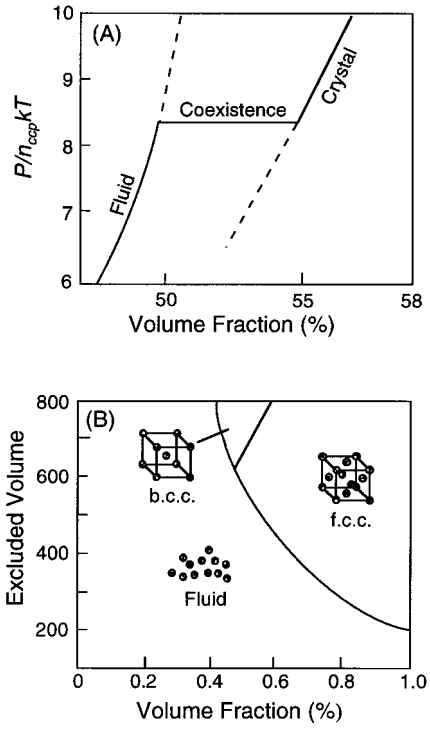

Fig. 8. Phase diagrams for colloidal systems whose constituent units are treated as A) hard, and B) soft spheres [9c]. The vertical axis of (A) represents the reduced pressure, which has been normalized by the thermal energy kT and the number density (n_{ccp}) of the ccp structure. As indicated in (A), hard spheres begin to order when they occupy approximately 50 % of the volume. This structural transition from a topologically disordered liquid into a long-range, highly ordered packing (the so-called Kirkwood–Alder transition) involves no change in heat or energy. It is solely driven by the entropic effect. The sedimentation of non-charged colloidal spheres can be treated according to the hard-sphere model, if the dispersion medium is non-polar and has a refractive index that nearly matches that of the colloidal spheres. As shown in (B), charged colloidal spheres can order into either bcc or fcc lattices as the volume fraction or the screening length increases. In either case, the disorder-to-order (or Kirkwood–Alder) transition occurs at much lower volume fractions than the hard-sphere system.

this method actually involves a strong coupling of several complex processes such as gravitational settling, translational diffusion (or Brownian motion), and crystallization (nucleation and growth). The success of this method relies on tight control over several parameters such as the size and density of the colloidal spheres, as well as the rate of sedimentation. The colloidal spheres can always settle completely to the bottom of a container as long as the size and density of these spheres are sufficiently high. Only when the sedimentation process is slow enough, the colloidal spheres concentrated at the bottom of the container will undergo a hard-sphere disorder-to-order phase transition (see the phase diagram in Fig. 8A) to form a three-dimensionally ordered lattice.[58] If the colloidal spheres are small in size (less than 0.5 μm) and/or their density is close to that of the dispersion medium, they will exist as a dispersed, equilibrium state in which the number of colloidal spheres per unit volume varies with height according to the Boltzmann distribution function.

Monodispersed silica colloids are most commonly employed in sedimentation due to the high density of amorphous silica. Opalescent structures (usually referred to as synthetic or artificial opals[11]) have been obtained from these colloidal materials under carefully controlled conditions.[59–61] It is generally accepted that the 3D crystalline arrays produced by this method have a cubic-close-packed (ccp) structure (or a face-centered-cubic (fcc) lattice with a packing density of ~74 %) similar to that of a natural opal.[59,62] The preference of a ccp structure over a hexagonal-close-packed (hcp) one has been suggested to be a result of the difference in entropy between these two structures.[63] Recently, van Blaaderen et al. demonstrated the use of lithographically defined surfaces as templates to grow 3D crystalline arrays with desired spatial structures.[64] This process is the mesoscopic equivalent of epitaxial growth: highly ordered and well-controlled arrays as large as ~1 cm^3 could be generated. Colvin and co-workers also developed a layer-by-layer sedimentation method for fabricating ccp arrays of silica colloids; these arrays have a tightly controlled number of layers along the [111] direction.[48]

The major disadvantage of the sedimentation method is that it has very little control over the morphology of the top surface and the number of layers of the 3D crystalline arrays.[65] Layered sedimentation may occur, which usually leads to the formation of a number of layers of different densities and orders along the direction of the gravitational field. It also takes relatively long periods of time (weeks to

  0935-9648/00/1005-0701 $ 17.50+.50/0

months) to completely settle submicrometer-sized particles. The 3D arrays produced by the sedimentation method are often polycrystalline in nature. Kumacheva and co-workers recently showed that sedimentation under an oscillatory shear could greatly enhance the crystallinity and ordering in the resulting 3D arrays.[66] In addition to its function as a means for increasing the concentration of colloidal spheres, the gravitational field may also have a profound effect on the crystalline structure. In a recent study, Chaikin and co-workers were able to eliminate this effect by performing the experiment on a space shuttle.[67] They found that the colloidal spheres were organized into a purely random hexagonal close packed (rhcp) structure at volume fractions up to 61.9 %.

4.2. Crystallization via Repulsive Electrostatic Interactions

Under appropriate conditions, highly charged colloidal spheres suspended in a dispersion medium can spontaneously organize themselves into a variety of crystalline structures as driven by minimization of electrostatic repulsive interactions. These ordered 3D arrays are usually referred to as colloidal crystals (Fig. 7B).[9,11] In 1988, Robbins and Grest noted that the phase diagram of such a colloidal suspension could be described using two thermodynamic variables: that is, the volume fraction of colloidal spheres and the electrostatic screening length (or the Debye–Hückel length, κ^{-1}) of the dispersion system.[68] The crystal structures that have been observed in this system include body-centered-cubic (bcc), fcc, rhcp, and AB_2.[9,69–71] Figure 8B shows a typical phase diagram for this system. When the screening length is shorter than the center-to-center distance between two spheres, the colloidal spheres act like "hard spheres" and they will not influence each other until they are in physical contact. In this case, a fcc crystal structure is formed, and no heat or energy change is involved upon crystallization. If the screening length is longer than the center-to-center distance, the colloidal spheres behave like "soft" spheres and will only crystallize into a bcc lattice, similar to that of a one-component plasma system.[71] In both crystalline structures, the colloidal spheres are separated by a distance comparable to their size. From the phase diagram, it is clear that the disorder-to-order transition can be provoked either by increasing the volume fraction of colloidal spheres or by extending the range of the screening length. A more recent synchrotron diffraction study indicated that charge-stabilized colloidal spheres could form fcc structures at all volume fractions up to ~60 %.[72,73]

The method based on repulsive electrostatic interactions seems to be the most powerful and successful route to large-scale 3D crystalline arrays of colloidal spheres. This method, however, has a very strict requirement on the experimental conditions: such as the temperature, monodispersity in size, density of charges on the surface of each sphere, number density of spheres, and concentrations of counterions in the dispersion medium. In most cases, a shear flow is necessary in order to form translational ordering over a long range.[74] The particles in the crystalline arrays formed by this method are always separated by a certain distance due to the repulsive interactions among these particles. Optimal fabrication of useful devices often requires an understanding how to control the crystalline structure by changing the interactions among colloidal spheres, as well as the kinetics of the colloidal spheres.

4.3. Self-Assembly under Physical Confinement

Monodispersed colloidal spheres often organize themselves into a highly ordered 3D structure when they are subjected to a physical confinement.[75] We recently demonstrated such a method (Fig. 7C) by which 3D opaline arrays of colloidal spheres could be produced with domain sizes as large as several square centimeters.[76] In this method, colloidal spheres (regardless of their surface and bulk properties) with a diameter ranging from 50 nm to 1 μm were assembled into a highly ordered structure in a specially designed packing cell. A continuous sonication was the key to the success of this method. Only under this condition was each colloidal sphere placed at the lattice site represented as a thermodynamic minimum. The 3D crystalline array was found to be in the ccp structure with a packing density very close to ~74 %, and the (111) face was parallel to the glass substrates. Figure 9 shows the SEM images of two typical examples. They were fabricated from electrically neutral polystyrene beads that were ~220 and ~480 nm in diameter. This method is relatively fast, and it also provides a tight control over the surface morphology and the number of layers of the crystalline assemblies. Because the opaline arrays formed by this method are three-dimensionally periodic structures, they can be directly used as tunable optical notch filters that are capable of selectively rejecting a very narrow wavelength interval of light (as determined by the Bragg equation) in the spectral region extending from ultraviolet to near infrared.[76b]

5. Template-Directed Synthesis of 3D Macroporous Materials

Template-directed synthesis is a convenient and versatile method for generating porous materials. It is also a cost-effective and high-throughput procedure that allows the complex topology present on the surface of a template to be duplicated in a single step. In this technique, the template simply serves as a scaffold around which other kinds of materials are synthesized. By templating against supermolecular assemblies self-organized from small molecules, surfactants, and block co-polymers, it has been possible to prepare various types of porous materials with pore sizes in

  0935-9648/00/1005-0702 $ 17.50+.50/0

ADVANCED MATERIALS

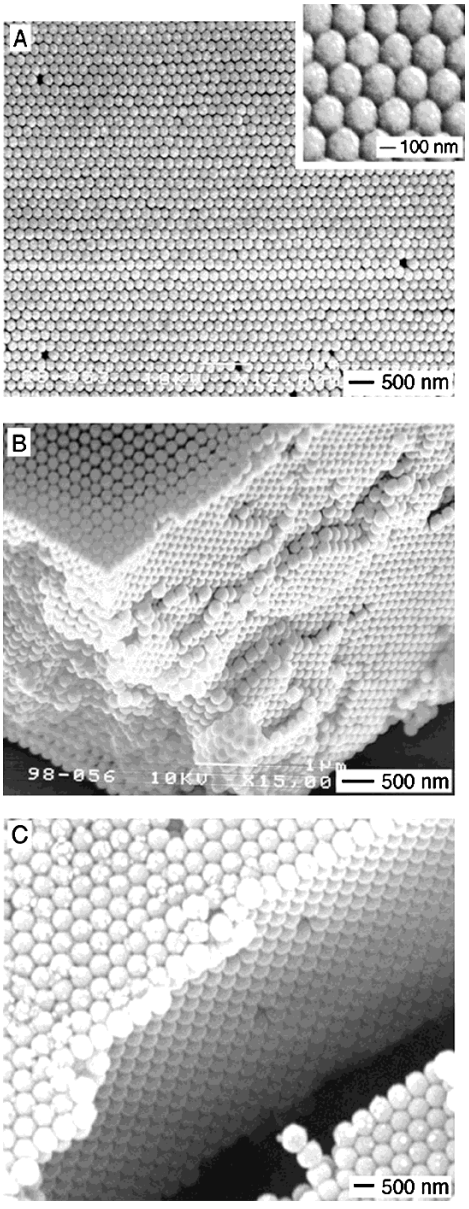

Fig. 9. SEM images of two 3D crystalline arrays that were assembled in 12 μm thick packing cells from: A,B) ~220 nm PS beads; and C) ~480 nm PS beads. By using such specially designed cells, it was possible to obtained highly ordered arrays over several square centimeters in area, with well-controlled numbers of layers along the [111] direction from one to a few hundred. These SEM images suggest that the ordering extends over all three dimensions, and could be assigned as a ccp structure [76].

the range of 0.3–10 nm.[77] With the use of mesoscale objects as templates, the dimension of these pores can be significantly extended to cover a wide range that spans from ~10 nm to 10 μm.[78] In particular, templating against opaline arrays of colloidal spheres offers a generic route to macroporous materials that exhibit precisely controlled pore sizes and highly ordered 3D porous structures.[79–81] Figure 10 illustrates the schematic procedure for this approach. After the opaline array of colloidal spheres has been dried, the void spaces (~26 % in volume) among the colloidal spheres are fully infiltrated with a liquid precursor

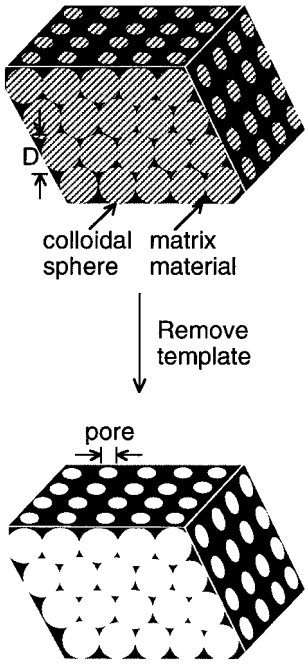

Fig. 10. Schematic outline of the experimental procedure that generates 3D porous materials by templating against crystalline arrays of colloidal spheres, followed by selective etching. Polystyrene beads and silica spheres are the two most commonly used templates. The polystyrene template can be removed either by calcination in air or by dissolution with toluene. The silica colloids are usually removed by etching with an aqueous HF solution.

such as an ultraviolet (UV) or thermally curable organic prepolymer,[80] an ordinary organic monomer (plus an initiator),[82] a sol–gel precursor to a ceramic material,[79–83] a solution containing an inorganic salt,[84] or a dispersion of nanoparticles with sizes in the range of 1–50 nm.[85] Subsequent solidification of the precursor and removal of the colloidal spheres gives a 3D porous structure that has a highly ordered architecture of uniform air balls (interconnected to each other by small circular "windows"). The void spaces among colloidal spheres have also been filled with a variety of materials through electrochemical deposition.[86] The fidelity of this procedure is mainly determined by van der Waals interactions, the wetting of the template surface, kinetic factors such as the filling of the void spaces in the template, and the volume shrinkage of precursors during solidification. The porous materials obtained by this approach have also been referred to as "inverse opals" or "inverted opals" because they have an open, periodic 3D framework complementary to that of an opaline structure.

Templating against opaline arrays of colloidal spheres has been successfully applied to the fabrication of 3D macroporous structures from a wide variety of materials, including organic polymers, ceramic materials, inorganic semiconductors, and metals.[79–88] Fabrication based on this approach is remarkable for its simplicity, and for its fidelity in transferring the structure from the template to the replica. The size of the pores and the periodicity of the porous structures can be precisely controlled and readily tuned by changing the size of the colloidal spheres. Table 2 gives a

  0935-9648/00/1005-0703 $ 17.50+.50/0

Table 2. Macroporous materials fabricated by templating against 3D colloidal arrays [a].

Template	Porous Materials	Precursors	Comments	Reference
Polymer beads	Polyurethanes, poly(acrylate-methacrylate) copolymers	UV-curable prepolymers (NOA, or SK-9)	Extraction with solvents, ordered [b]	[80]
	Au	Gold nanoparticles	Extraction with solvents, partially ordered [b]	[85c]
	Ni, NiO	$(CH_3CO_2)_2Ni$	Calcination, partially ordered	[84]
	SiO_2	Snowtex Zl and OL	Calcination, ordered	[85b]
	TiO_2	Titania nanoparticles	Calcination, ordered	[85b,91]
	SiO_2, TiO_2, ZrO_2, $Al_2O_3{\cdot}H_2O$, WO_3, Fe_2O_3, Sb_4O_6, $Y_{0.043}Zr_{0.957}O_2$, $AlPO_4$, Nb_2O_5, Vinyl or cyano functional silicates	Metal alkoxides and metal chlorides	Calcination or extraction with solvents, ordered or partially ordered	[78c,79a,79b,80c, 81a,81b,83,88,89a, 89b]
Silica colloids	Organic polymers	Organic monomers	HF etch, ordered and partially ordered	[80c,82,86a,90,119]
	Carbon	Thermally cured phenolic resin, or chemical vapor deposition	HF etch, ordered	[87]
	Ni, Cu, Ag, Au, Pt	Electroless deposition on gold nanoparticles	HF etch, ordered	[86a]
	CdS, CdSe	$CdSO_4$, SeO_2	HF etch, ordered	[86b]
	CdSe	CdSe nanoparticles	HF etch, ordered	[85a]
Emulsion templating	Poly(acrylamide)	$H_2C{=}CHCONH_2$ and $(H_2C{=}CHCONH)_2CH_2$	Drying, disordered	[78d]
	SiO_2, TiO_2, ZrO_2	Metal alkoxides	Drying, calcination, disordered	[78b,78d]

[a] Information contained here is in accordance with our knowledge of related publications at this time. [b] Ordered refers to long-range order within the sample. Partially ordered refers to smaller domain sizes.

partial list of such 3D porous materials that have been fabricated and characterized. There is no doubt that a similar approach is extendible to other materials. The only requirement seems to be the availability of a precursor that can infiltrate into the void spaces among colloidal spheres without significantly swelling or dissolving the template (usually made of polystyrene beads or silica spheres). Some gaseous precursors have also been employed in this process albeit the initial product deposited on the surfaces of samples might block the flow in of gaseous precursors.[87] At present, the smallest colloidal spheres that have been successfully used in this method are ~35 nm in diameter;[82] the lower limit to the particle size that can be incorporated into this technique has not been completely established. Recently, Stucky and co-workers demonstrated a simple and convenient method for fabricating hierarchically porous materials by combining colloidal arrays and block copolymers into a single system.[88]

Figure 11 shows SEM images of several typical examples of 3D porous materials that were fabricated by our research group: macroporous thin films of polyurethane, SiO_2, SnO_2, and TiO_2.[80] As illustrated by these images, these membrane-type films have a periodic structure complementary to that of an opal—each of them consists of a highly ordered, 3D array of uniform air balls that are interconnected to each other by a small "window". For organic polymers, it has been possible to fabricate such 3D porous structures as free-standing thin films that are several square centimeters in area.[80c] These porous membranes can be subsequently incorporated into a flow system to measure and study the permeabilities of various kinds of gases and liquids. For metals and ceramic materials, the porous struc-

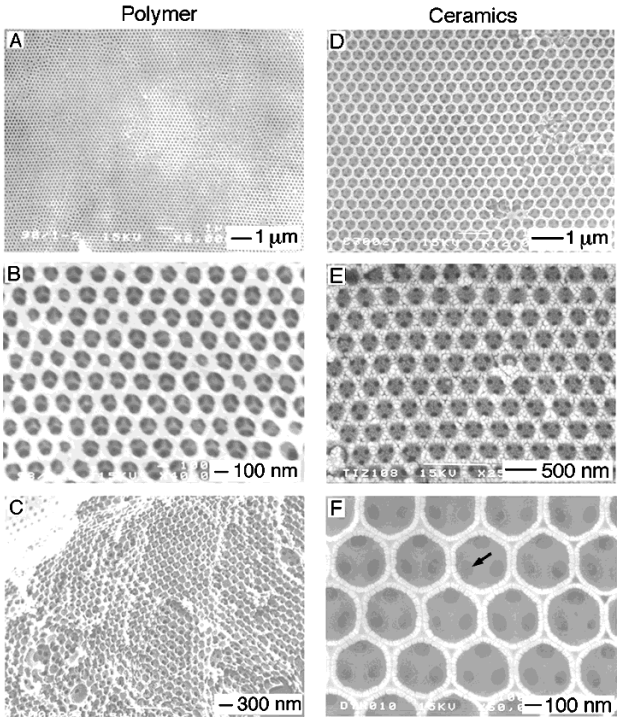

Fig. 11. SEM images of 3D porous materials that were made of: A–C) polyurethane; D) SiO_2; E) SnO_2; and F) TiO_2 [80]. They were fabricated by templating a UV-curable prepolymer (A–C) and sol–gel precursors (D–F) against crystalline arrays of polystyrene beads, followed by etching in toluene. The images of (A–C) were taken from the same film, and C) shows a cross-sectional view of the sample. It can be clearly seen that each spherical pore is connected to 12 adjacent spherical pores by 12 small circular windows, as indicated by an arrow. The dimensions of these windows is largely determined by the degree of physical contact between adjacent colloidal spheres, and the amount of liquid precursor infiltrated into the void spaces.

  0935-9648/00/1005-0704 $ 17.50+.50/0

ADVANCED MATERIALS

tures still remain too fragile to be released from their solid supports. The high percentage of volume shrinkage involved in the solidification of these inorganic materials (in particular for sol–gel precursors) usually results in random cracks in these thin films.

Although this templating procedure may lack the characteristics required for high-volume production, it does provide a simple and effective route to 3D porous materials having tightly controlled pore sizes and well-defined periodic structures. These porous structures can serve as unique model systems to study many interesting subjects such as adsorption, condensation, transport (diffusion and flow), and separation of molecules in macroporous materials, as well as mechanical, thermal, and optical properties of 3D porous materials. With appropriate surface modifications, these 3D open structures (porosity (74 %) should also be useful for fabricating prototype sensors with enhanced sensitivities, or as templates to generate complex 3D structures of various functional materials that can not be produced using conventional lithographic techniques. Because of their long-range ordering, these 3D periodic structures are particularly promising as PBG crystals that may exhibit complete bandgaps in the spectral regime that covers the UV, through visible, to near-infrared (see Sec. 6.3).[89–91] Other types of applications that have been proposed for these 3D macroporous materials include their potential usage as collectors of solar energies, as model systems for studying quantum confinement, as electrodes for fuel cells and other types of electrochemical processes, as supports for catalysts, and as low-dielectric materials for capacitors.

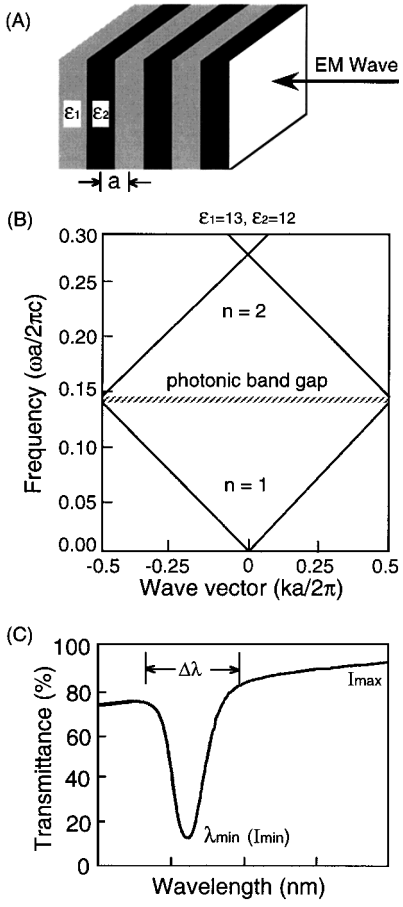

Fig. 12. A) Illustration of a 1D PBG crystal made of alternating thin layers of two dielectric materials. B) The photonic band structure (normal incidence) calculated for a typical 1D PBG crystal where ε_1 and ε_2 are equal to 13 and 12, respectively. The dashed region indicates the photonic bandgap. Any electromagnetic wave whose frequency falls anywhere in this gap cannot propagate through this PBG crystal. C) The photonic band structure of a PBG crystal can be probed experimentally by measuring its transmission spectra using electromagnetic waves with different wavelengths. The bandgap is usually characterized by three parameters: the position of the midgap (λ_{min}), the width of the gap ($\Delta\lambda$) or the gap/midgap ratio ($\Delta\lambda/\lambda_{min}$), and the maximum attenuation of the gap ($10\log(I_{max}/I_{min})$ in the unit of dB) [92].

6. Fabrication of PBG Crystals from Colloidal Spheres

A PBG crystal (or photonic crystal) is a spatially periodic structure fabricated from materials having different dielectric constants.[92] It can influence the propagation of electromagnetic waves in a similar way as a semiconductor does for electrons—that is, there exists a bandgap that excludes the passage of photons of a chosen range of frequencies (Fig. 12). The concept of this new class of material was first proposed independently by Yablonovich[93] and John[94] in 1987, and since then a wide variety of applications has been envisioned or demonstrated for this new class of material. A photonic crystal, for example, provides a convenient and powerful tool to confine, control, and manipulate photons in all three dimensions of space: for example, to block the propagation of photons irrespective of their polarization or direction; to localize photons to a specific area at restricted frequencies; to inhibit the spontaneous emission of an excited chromophore; to modulate or control stimulated emission; and to serve as a lossless waveguide to direct the propagation of photons along a specific direction.[95,96] All of these photonic properties are technologically important because they can be exploited, in principle, to produce light-emitting diodes (LEDs) that display coherence properties, to fabricate thresholdless semiconductor diode lasers, and to significantly enhance the performance of many other types of optical, electro-optical, and quantum electronic devices.

Research on PBG crystals has extended to cover all three dimensions, and the spectral region ranging from ultraviolet to radio frequencies. The real push in this area, however, has been the strong desire to obtain a 3D bandgap around 1.55 μm—the wavelength now used in optical fiber communications. Through an interplay between computational simulation and experimentation, the goal has now been successfully accomplished to produce one-, two-, and three-dimensional bandgaps for microwave and millimeter-wave radiations.[95–97] For wavelengths shorter than near-infrared, true photonic gaps have only been achieved in one- and two-dimensional systems, although computational studies have pointed out the conditions (e.g., the crystal

  0935-9648/00/1005-0705 $ 17.50+.50/0

structure, the shape of the building block, the minimum contrast between the high and low dielectric regions, and the lattice parameter) under which a 3D photonic crystal will display a complete gap in the optical regime.[98] The fundamental challenge at present is one of materials science: that is, the fabrication of such 3D structures in a controllable way and at a reasonable cost. At the current stage of development, it is still difficult to apply conventional microlithographic techniques to the fabrication of 3D periodic structures that meet all the proposed criteria when the feature size becomes comparable to the wavelength of near-infrared or visible light. Nevertheless, a number of 3D structures amenable to layer-by-layer fabrication or patterning have already been generated in prototype forms and are expected to display complete 3D bandgaps in the optical regime.[99] An alternative route to 3D periodic structures is based on self-assembly in which building blocks are spontaneously organized into stable, well-defined structures by non-covalent forces.[100] The key idea in self-assembly is that the final structure is close to or at thermodynamic equilibrium; it thus tends to reject defects. A wide variety of self-assembling strategies have been successfully demonstrated for fabricating three-dimensionally ordered structures with feature size ranging from molecular, through mesoscopic, to macroscopic scales. Those that have been explored for making 3D photonic crystals include phase separation of block co-polymers,[101] crystallization of monodispersed colloidal spheres,[102] and template-directed synthesis.[89–91] Next we will concentrate on the last two approaches; both of them involve the use of monodispersed colloidal spheres as the building blocks.

6.1. Search for 3D PBGs

A complete (or full, true) gap is defined as one that extends throughout the entire Brillouin zone in the photonic band structure.[92] An incomplete one is often referred to as a pseudo gap (or the so-called stop bandgap), because it only shows up in the transmission spectrum along a certain propagation direction. A 3D complete gap can thus be considered as a stop band that has a frequency overlap in all three dimensions of space. For a 1D system (Fig. 12),[92] there always exists an infinite number of full gaps in the band structure as long as there exists a dielectric contrast. For a 2D or 3D system, however, the evolution of a full bandgap strongly depends on the crystal structure, as well as the dielectric contrast (i.e., the strength of the potential well).[95–99] In principle, the band structure of a PBG crystal can be obtained by solving the Maxwell equations that contain a spatially periodic function for the dielectric constant. Because the Maxwell equations enjoy scale invariance, one can shift a gap theoretically to any frequency range by scaling all the sizes of a given periodic structure. A number of techniques have already been demonstrated for calculating photonic band structures of various types of PBG crystals. The plane wave expansion method (PWEM) seems to be the most commonly used tool for 3D systems, albeit it cannot be applied to those systems whose dielectric constants exhibit large imaginary parts.[103] A viable alternative to this method is the photonic analogue of the Korringa–Kohn–Rostoker (KKR) approach, which has been able to produce results similar to those obtained by the PWEM.[104] The traditional scalar-wave approximation, on the other hand, has been found to be inadequate in fully describing many important aspects of 3D photonic crystals.[105]

Theoretical studies that involve 3D systems have been largely focused on the fcc structure because the Brillouin zone of this lattice has the least derivation from a sphere and thus appears to be favored for the formation of a PBG. A detailed description of the computational results was recently summarized by Busch and John[98b] and Haus.[106] For a fcc lattice consisting of colloidal spheres, there only exists a pseudo gap in the photonic band structure, no matter how high the dielectric contrast.[106,107] The existence of a complete gap in this simple system is inhibited by a symmetry-induced degeneracy at the W-point. When the symmetry of such a fcc lattice is reduced to a diamond structure, a true gap evolves between the second and third bands in the photonic band structure, with a maximum gap/midgap ratio of ~15.7 % located at a volume fraction of ~37 % and a dielectric contrast of ~13 (or ~3.6, in terms of refractive index).[98] The symmetry-induced degeneracy at the W-point can also be lifted by choosing non-spherical objects as the building block to form the fcc lattice.[107] Gu and co-workers have theoretically shown that a full gap (between the second and third bands) can develop in the photonic band structure when the building block is a dimeric object consisting of two dielectric spheres interconnected to each other.[108] This full bandgap has a width of ~11.2 % for a volume fraction of ~30 % and a dielectric contrast of ~13. Recent calculations also suggested that the stop band of a fcc lattice could be significantly widened or fully opened by using colloidal spheres made of materials with large magnetic susceptibilities or intensity-dependent refractive indices.[109]

Cubic lattices consisting of interconnected air balls embedded in a continuous dielectric matrix (i.e., inverse opals) represent another promising structure type that might exhibit a complete 3D bandgap.[98,110] Theoretical studies indicate that the minimum contrast between the refractive indices at which a complete gap (between the eighth and ninth bands) is formed depends on the structural type and varies from 1.9 for a layered structure, through ~2.1 for a diamond structure, to ~2.8–2.9 for a fcc inverse opal structure. In the fcc case, a gap/midgap ratio as large as ~14 % can be achieved. More recently, Busch and John showed that an inverse opal can also display a fully tunable bandgap if the surface of the 3D porous structure is coated with an optically birefringent nematic liquid crystal.[110] This 3D bandgap can be opened or closed by applying an

  0935-9648/00/1005-0706 $ 17.50+.50/0

electric field that rotates the axis of the liquid crystal molecules with respect to the backbone of the inverse opal. Inverse opals with a hcp structure of air balls also exhibit complete bandgaps if the dielectric contrast is sufficiently high.[98b]

6.2. Crystalline Arrays of Colloidal Spheres as 3D Photonic Crystals

Although crystalline arrays of colloidal spheres are not expected to exhibit full bandgaps due to the relatively low dielectric contrast that can be achieved for these materials, they offer a simple and easily prepared model system to experimentally probe the photonic band diagrams of certain types of 3D periodic structures.

Colloidal crystals[11] assembled from highly charged polystyrene beads or silica spheres have been known for a long time to produce Bragg diffraction of light in the optical region.[111] Spry and Kosan and Asher and co-workers noticed that the position, width, and attenuation of the Bragg diffraction peak could be described by the dynamic scattering theory that was originally put forward by Zachariasen for X-ray diffraction.[112] These highly ordered systems were recently, studied in more detail as photonic crystals by Vos et al.,[113] Watson and co-workers,[114] and several other groups. Vos et al. also concluded that the dynamic scattering theory had to be modified to take into account the excluded volume effect.[115]

Lopez and co-workers,[116] Vlasov and co-workers,[117] Zhang and co-workers,[118] and Colvin and co-workers[119] have extensively investigated the photonic properties of artificial opals[11] fabricated from monodispersed silica colloids. In some cases, the void spaces among the colloidal spheres could be infiltrated with a variety of other materials to change the dielectric contrast.[120] Colvin and co-workers also measured the dependence of stop band attenuation on the number of layers along the [111] direction.[119] Our group studied the photonic properties of opaline structures assembled from polystyrene beads.[76,121] Figure 13A shows the photograph of such a PBG crystal that contains a set of bands with different colors. Each color band corresponds to a 3D crystalline array formed from PS beads of a specific size: 270 nm for the red color, 220 nm for the green color, and 206 nm for the blue color.[121b] All of these PS beads were essentially uncharged on their surfaces and the resulting crystals had a ccp structure. Figure 13B gives the UV-vis transmission spectra that were obtained from the red-, green-, and blue-colored regions of the sample. In principle, it should also be straightforward to incorporate a large number of different PS beads into the same photonic crystal. By simply scanning across the surface of this sample, one should have access to photonic crystals that display a wide range of different stop bands. Figure 13C illustrates the dependence of the position of stop band on the size of PS beads. Obviously, the

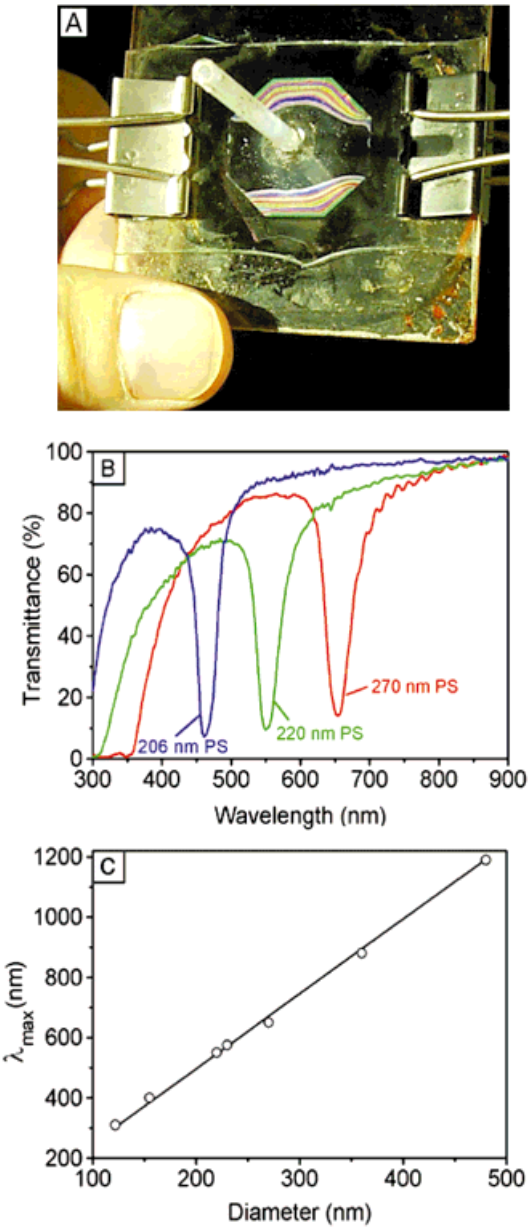

Fig. 13. A typical 3D PBG crystal fabricated from monodispersed PS beads [121]. A) A photograph of the cell that was used to assemble PS beads into a crystalline structure consisting of a set of colored bands. The red-, green-, and blue-colored regions are all ccp lattices made of 270, 220, and 206 nm PS beads, respectively. B) The UV-vis transmission spectra obtained from each colored region. C) The linear relationship between the midgap position and the size of the PS beads.

position of the stop band can be changed to cover the whole spectral region from UV to near-IR by choosing PS beads with different diameters. All of these studies are consistent with the computational results: that is, there only exists a pseudo bandgap for any fcc lattice self-assembled from monodispersed colloidal spheres. More recently, Lopez and co-workers and Xia and co-workers demonstrated the capability to fine tune the stop band of the 3D crystalline array fabricated from PS beads or silica colloids by sintering the samples to elevated temperatures.[122,123] In this

  0935-9648/00/1005-0707 $ 17.50+.50/0

case, the position (and intensity) of the stop band could be changed in a controllable way to cover a narrow spectral region.

6.3. Inverse Opals as 3D Photonic Crystals

Computational studies have suggested that a porous material consisting of a opaline lattice of interconnected air balls (embedded in an interconnected matrix with a higher refractive index) should give rise to a complete gap in the 3D photonic band structure.[98b] Optimum photonic effects require the volume fraction of the matrix material to fall anywhere in the range of 20–30 %. Although such a 3D structure can be built up layer by layer through conventional microlithographic techniques, it has been very difficult to achieve that goal when the feature size becomes comparable to the wavelength of visible light.[124] Processing difficulties have also limited the formation of such 3D structures with more than a few layers, or from materials other than those currently employed in microelectronics. An alternative approach is based on template-directed synthesis against opaline arrays of colloidal spheres (see Sec. 5). This method is attractive because the periodicity of this system can be conveniently tuned and a wide variety of materials with relatively high refractive indices can be easily incorporated into the procedure (see Table 2).

The most promising candidates for the matrix seem to be some wide bandgap semiconductors such as diamond, II–VI semiconductors (e.g., CdS and CdSe), titania, and tin dioxide because they have a refractive index higher than 2.5 and are optically transparent in the visible and near-IR region.[125] Other semiconductors with strong absorption in the visible region (such as Si and Ge) can be applied to the near-IR regime. Since the first demonstration by Velev et al. in 1997, many advances have recently been made in this area.[79a] For instance, Vos and co-workers have demonstrated the fabrication with polycrystalline titania (anatase) by using a sol–gel process and also measured the reflectance spectrum of this crystal.[89] Baughman and co-workers have incorporated chemical vapor deposition (CVD) into this procedure and generated inverse opals containing different forms of carbon.[87] Norris and co-workers and Braun and Wiltzius were able to obtain 3D periodic structures from II–VI semiconductors such as CdS and CdSe, albeit no optical measurement was presented in their publications.[85a,86b] Stein and co-workers, Velev et al., and Colvin and co-workers also fabricated highly ordered 3D porous materials from metals that might display interesting photonic properties.[84,85c,86a] Pine and co-workers and Subramania et al. have fabricated inverse opals of titania by filling the void spaces among colloidal spheres with slurries of nanometer-sized titania particles.[85b,91] They also observed stop bands (between the second and third bands) for these 3D porous materials made of rutile- and anatase-phase titania. Despite these advances, a definitive signature of the existence of a complete photonic bandgap is still missing for these 3D porous materials. Part of the reason lies in the fact that the filling of the void spaces was not complete in most cases and the resulting materials might not be dense enough to acquire a refractive index close to that of the bulk material. For example, Vos and co-workers have estimated the refractive index of their anatase porous structure to be 1.18–1.29, a value that is much lower than that of single crystalline bulk anatase (~2.6).[89]

7. Other Applications of Crystalline Arrays of Colloidal Spheres

Crystalline arrays of colloidal spheres have also attracted considerable attention for their unique applications in many other areas. For instance, they have been extensively exploited as a model system with which to study the mechanisms of structural phase transitions.[126] In some cases, these transitions can mimic the complex, many-body properties of condensed matter on the atomic scale. The long time scale of the motion of colloids allows one to make real time observation and analysis of various phenomena, which are difficult or impossible to achieve for atomic and molecular systems. Crystalline arrays of colloidal spheres also provide a potentially useful route to high-strength ceramics.[127] In this approach, ceramic materials are produced as uniform colloidal spheres and subsequently crystallized into closely packed lattices so that all grains and pores are the same size. As we are limited by space, next we will only describe two more applications that are based on crystalline arrays of monodispersed colloidal spheres.

7.1. 2D Crystalline Arrays of Colloidal Spheres as Masks in Lithography

When colloidal spheres form a two-dimensional, closely packed, hexagonal array on the surface of a solid substrate, there exists a triangular void space among the three spheres that are in physical contact to each other. This ordered array of void spaces can serve as a physical mask through which other materials such as metals or dielectric materials can be selectively deposited onto the surface of the underlying substrate using ordinary lift-off procedures that involve vacuum evaporation or sputtering. This method for generating patterned arrays of microfeatures (usually as discrete dots) was initially referred to as "natural lithography",[128] and more recently as "nanosphere lithography".[50] Figure 14 shows the schematic diagram of such an approach. The deposited material forms a hexagonal array of dots on the solid support. Each dot has the geometry of the largest inscribed equilateral triangle. One of the most attractive features of this technique is that the lateral dimension of the resulting structures is only about one seventh of the diameter of the colloidal spheres. As a result, it is relatively easy and

  0935-9648/00/1005-0708 $ 17.50+.50/0

ADVANCED MATERIALS

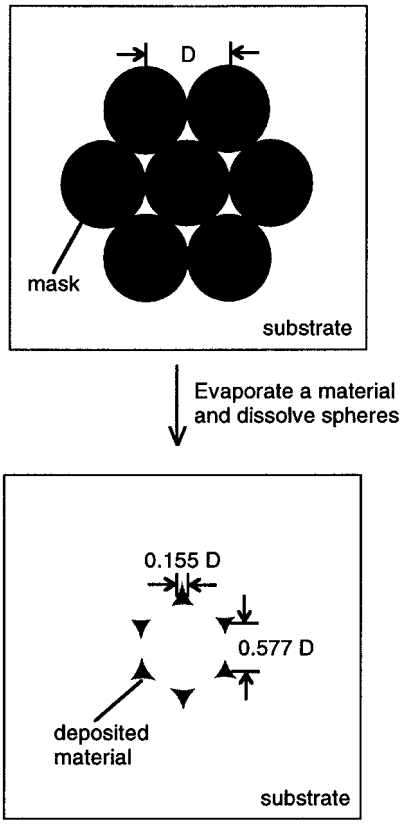

Fig. 14. Schematic illustration of "nanophase lithography" in which a 2D hexagonal array of colloidal spheres is used as the physical mask for selective deposition. After the colloidal spheres have been removed, a regular 2D array of nanofeatures is left behind on the surface of the substrate [50].

straightforward to produce regular arrays of isolated nanostructures from micrometer-sized colloidal spheres using this method. If the colloidal spheres are robust enough to resist energetic species, the triangular voids in the 2D array of colloidal spheres can be transferred directly into the surface of a substrate by using dry processes such as reactive ion etching (RIE) or argon ion milling.[129] If the colloidal spheres are chemically linked to the surface of a substrate, it might also be possible to achieve pattern transfer by using solution-phase deposition or wet etching.

Since its first demonstration by Fisher and Zingsheim in the early 1980s,[130] this lithographic method has been explored by a number of groups for generating 2D arrays of nanostructures from a variety of materials in (or supported on) the surfaces of solid substrates: Fisher and Zingsheim demonstrated the fabrication of 2D arrays of Pt dots on glass substrates by lift-off.[130] Deckman and Moustakas fabricated 2D arrays of Si and GaAs posts by reactive ion milling and 2D arrays of Ag dots by lift-off.[131] Roxlo et al. employed this method to texture the surface of MoS_2, a layered compound having catalytic activities.[129,132] Buncick et al. fabricated 2D arrays of Ag ellipsoidal particles using this method and studied their optical properties.[133] Fang et al. and Green et al. fabricated quantum pillar structures in the surfaces of GaAs substrates.[134] Dozier et al. fabricated high-T_c Josephson effect devices in YBCO thin films.[135] Lenzmann et al. fabricated 2D arrays of ZnS hemispheres by lift-off, followed by thermal growth.[43b] Burmeister and co-workers patterned the surfaces of substrates such as glass, ITO, and WSe_2.[136] Wiesendanger et al. formed 2D arrays of magnetic nanoparticles using this method and characterized these arrays by scanning probe microscopy.[137] Van Duyne and co-workers systematically studied this lithographic method. They extended it to micropatterning of molecular materials, and also introduced the use of double-layered arrays of polystyrene beads in masked evaporation of silver.[50] Douglas et al. extended the resolution of this method to the scale of ~10 nm by making 2D arrays of spheres from protein molecules (the so called S-layer).[138]

"Nanosphere lithography" is an intrinsically parallel process. It also provides a simple, convenient, low-cost, and materials-general method for generating 2D arrays of nanostructures from a broad range of materials on the surfaces of a wide variety of substrates. The patterned nanostructures fabricated using this method are useful in a number of areas—for example, to serve as antireflection coatings, regular arrays of microelectrodes, and selective solar absorbers; to function as active layers to enhance Raman scattering or to improve photovoltaics; to work as supports in biosensing or heterogeneous catalysis, and to perform as arrays of quantum dots or single-electron transistors. The major problem that hinders the use of this method in practice is the lack of a tight control over the density of defects (point defects and dislocations), and the size of domains. Also, in the original setup of this approach, it is difficult to change the lateral dimensions of the features and the separation between these features independently.

7.2. 3D Crystalline Arrays of Colloidal Spheres as Optical Sensors

A 3D crystalline array of colloidal spheres can strongly diffract light of a specific wavelength as determined by the Bragg condition:[111]

$$m\lambda_{\min} = 2nd_{hkl}\sin\theta \quad (2)$$

where m is the order of the diffraction, $\lambda_{\min}$ is the wavelength of the diffracted light (or the so-called stop band), n is the mean refractive index of the 3D array, d_{hkl} is the interplanar spacing along the [hkl] direction, and θ is the angle between the incident light and the normal to the (hkl) planes. This equation indicates that the position of the stop band is directly proportional to the interplanar spacing. Any variation in the spacing should result in a observable shift in the diffraction peak. As a result, a 3D array of colloidal spheres can serve as an optical sensor that is capable of displaying and measuring environmental changes (Fig. 15). Optical sensors can thus be fabricated by combin-

  0935-9648/00/1005-0709 $ 17.50+.50/0

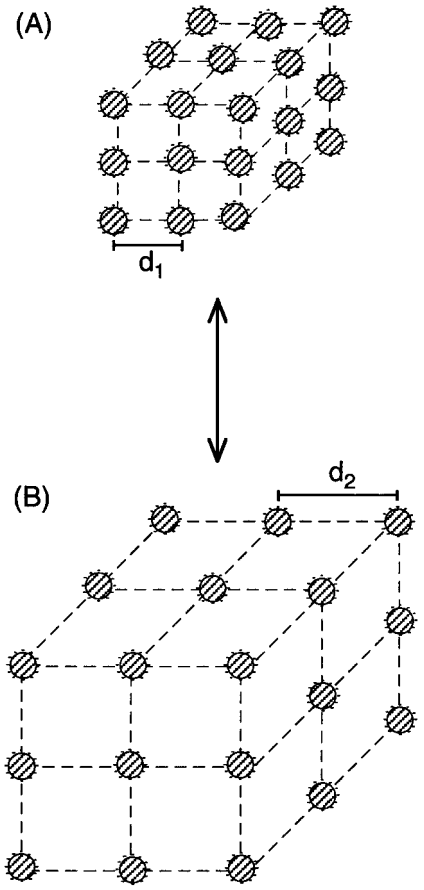

Fig. 15. Schematic illustration of sensing protocol that involves 3D crystalline arrays of colloidal spheres [140]. When the array is exposed to an analyte (or change in temperature), the spacing between colloidal spheres may change accordingly. Depending on the position of the Bragg diffraction peak, this small change in lattice constant can be easily visualized by the naked eye or observed using a spectrometer.

ing the responsiveness of polymer gels (or other kinds of functional materials) to environmental stimuli with the diffractive power of 3D colloidal arrays.

A number of smart sensors have been demonstrated through the work of Asher and co-workers.[139,140] In their work, highly charged colloidal spheres were assembled into 3D colloidal crystals with lattice constants in the range of 50–500 nm. Embedding the crystalline array in a polymer matrix helps to retain its ordered structure when exposed to varying environments. Two diffractive devices sensitive to temperature changes have been fabricated from poly(*N*-isopropylacrylamide) (PNIPAM), which reversibly dehydrates and thus changes its conformation with a moderate change in temperature.[141] When the colloidal spheres are made of PNIPAM, a variation in temperature changes the diameter of the colloidal spheres and leads to a modification in the intensity of the Bragg diffraction peak.[139] When the matrix around polymer beads is made of PNIPAM, the reversible shrinkage of this material between 10–35 °C changes the lattice spacing and subsequently results in a shift of the Bragg diffraction peak.[139] Chemically responsive colloidal crystals have also been demonstrated. For example, a hydrogel responsive to Pb^{2+}, Ba^{2+}, and K^+ was fabricated by incorporating crown-ether (4-acryloyl aminobenzo-18-crown-6) groups into the gel matrix.[140] The crown ethers selectively trapped these cations, drawing in counterions, increasing the Donnan osmotic pressure of the hydrogel, and swelling the matrix. The magnitude of this reversible swelling depended on the number of charged groups covalently attached to the gel. An ~150 nm red shift was observed when the concentration of Pb^{2+} was increased from ~20 ppb to ~2000 ppm. In another demonstration, an enzymatic-based glucose sensor was also demonstrated with reversible swelling in response to the presence of 10^{-12} M (in the absence of O_2) to 0.5 mM glucose. The avidine-functionalized enzyme glucose oxidase was attached to a biotinylated composite of crystalline colloidal spheres in a polyacrylamide gel.[140] Conversion of glucose to gluconic acid by the enzyme swells the gel via the formation of anions, increasing the lattice spacing of the crystalline framework. Sensing devices have also been fabricated by placing a stabilized crystalline array of colloidal spheres at the end of an optical fiber. The optical sensors fabricated using this approach are potentially useful in a number of areas such as clinical diagnostics and environmental monitoring.

8. Summary and Outlook

Monodispersed colloidal spheres have emerged as the material of choice for a wide variety of niche applications that range from nanopatterning to fabrication of photonic devices. These materials may represent the simplest class of building blocks that can be readily assembled into three-dimensionally ordered structures—colloidal crystals and opaline arrays.[11] Furthermore, new types of 3D periodic structures (e.g., inverse opals) can also be easily fabricated by templating various kinds of precursors against crystalline arrays of colloidal spheres. These two simple approaches provide a flexible and cost-effective route to high-quality, 3D structures with remarkably little of the investment required by the more familiar clean-room methods commonly used in microfabrication. The feature size of these highly ordered structures can also be easily varied in a well-controlled way to cover an extremely broad range that spans from a few nanometers to a few hundred micrometers. The ability to generate such periodic 3D structures with varying feature sizes allows one to obtain useful functionalities not only from the constituent materials but also from the long-range ordering that characterizes these structures. For example, both colloidal arrays and inverse opals can be exploited as a platform to fabricate novel types of optical or electro-optical devices such as photonic crystals and smart diffractive sensors.

Monodispersed colloidal spheres and most of the applications derived from these materials are still in an early stage of technical development. There are a number of issues that remain to be addressed before these materials can reach their potential in core industrial applications. First, the di-

  0935-9648/00/1005-0710 $ 17.50+.50/0

ADVANCED MATERIALS

versity of materials must be greatly expanded to include every major class of functional material. Currently, only silica and a few polymers (e.g., PS and PMMA) have been prepared as truly monodispersed colloidal spheres. These materials, however, do not exhibit any particularly interesting optical, nonlinear optical, or electro-optical functionality. Second, formation of complex crystal structures other than ccp, bcp, and rhcp lattices has to be demonstrated. As a major limitation to the self-assembly approaches described in this review, all of them are not capable of generating arbitrary 3D structures. Recent demonstrations based on optical trapping may provide a potential solution to this problem, albeit this approach might be too slow to be useful in practice.[56,57] Another potentially useful approach is based on the self-assembly of polydispersed colloidal spheres having a well-defined distribution in size.[142] Third, the density of defects in the crystalline arrays of colloidal spheres must be well-characterized and kept below the level tolerated by a certain type of photonic application. Fourth, the compatibility of the crystallization techniques with the processes used in the production of other types of integrated electro-optical devices (such as diode lasers) still needs to be defined and improved.

Monodispersed colloidal spheres will, of course, continue as the dominant subject of research in colloid science. They are, however, not necessarily the best and/or the only option for all fundamental studies and applications that involve the use of colloidal particles. They are not, for example, suitable building blocks for generating 3D PBG crystals with complete bandgaps.[98] Non-spherical colloidal particles may offer some immediate advantages over their spherical counterparts in applications that require periodic structures with lower symmetries. Colloidal cubes, ellipsoids, and rods have been directly synthesized using a rich variety of chemical methods, but none of these samples was truly monodispersed in size and/or shape.[8,143] Two indirect approaches seem to be more promising in this regard, both of them are based on monodispersed colloidal spheres. In the first method, monodispersed PS beads were swollen with an immiscible monomer with the help of an aprotic solvent. Subsequent polymerization of the new monomer led to the formation of peanut-shaped colloidal particles due to the phase separation effect.[144,145] Figure 16 shows the SEM image of such particles that were fabricated from PS and PMMA.[146] In the second method, monodispersed PS or PMMA spheres were embedded in a polymer matrix and subsequently converted into ellipsoids during a thermal-stretching process.[147,148] These non-spherical particles will certainly provide complexity and new types of functionalities that can not be offered by spherical colloids.

Received: February 25, 2000

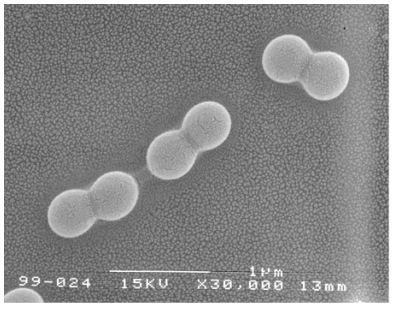

Fig. 16. The SEM image of several peanut-shaped colloidal particles that were synthesized by swelling monodispersed PS beads (480 nm in diameter) with an MMA (methylmethacrylic acid) monomer, followed by radical polymerization of the MMA into a polymer, PMMA. The PMMA phase was separated from the PS sphere during the polymerization process to form a peanut-shaped dimer consisting of two spheres: one is PS and the other is PMMA [146].

[1] a) D. H. Everett, *Basic Principles of Colloid Science*, Royal Society of Chemistry, London **1988**. b) W. B. Russel, D. A. Saville, W. R. Schowalter, *Colloidal Dispersions*, Cambridge University Press, Cambridge **1989**. c) R. J. Hunter, *Introduction to Modern Colloid Science*, Oxford University Press, Oxford **1993**. d) *Ordering and Phase Transitions in Colloidal Systems* (Eds: A. K. Arora, B. V. R. Tata), VCH, Weinheim **1996**.

[2] *Microscopy & Histology Catalog*, Polysciences, Warrington, PA **1993**–**1994**.

[3] Reviews on metal colloids: a) A. Henglein, *Chem. Rev.* **1989**, *89*, 1861. b) G. Schmid, *Chem. Rev.* **1992**, *92*, 1709. c) G. Schon, U. Simon, *Colloid Polym. Sci.* **1995**, *273*, 101. d) Z. L. Wang, *Adv. Mater.* **1998**, *10*, 13. e) G. Schmid, L. F. Chi, *Adv. Mater.* **1998**, *10*, 515.

[4] Reviews on semiconductor nanocrystallites: a) M. L. Steigerwald, L. E. Brus, *Acc. Chem. Res.* **1990**, *23*, 183. b) M. G. Bawendi, M. L. Steigerwald, L. E. Brus, *Annu. Rev. Phys. Chem.* **1990**, *41*, 477. c) Y. Wang, *Acc. Chem. Res.* **1991**, *24*, 133. d) H. Weller, *Angew. Chem. Int. Ed. Engl.* **1993**, *32*, 41. e) A. P. Alivisatos, *Science* **1996**, *271*, 933.

[5] General reviews on nanophase materials: a) J. H. Fendler, *Chem. Rev.* **1987**, *87*, 877. b) G. A. Ozin, *Adv. Mater.* **1992**, *4*, 612. c) *Nanophase Materials: Synthesis, Properties, Applications* (Eds: G. C. Hadjipanayis, R. W. Siegel), Kluwer Academic, Norwell, MA **1994**. d) D. A. Tomalia, *Adv. Mater.* **1994**, *6*, 529.

[6] R. K. Iler, *The Chemistry of Silica*, Wiley, New York **1979**.

[7] a) *Emulsion Polymerization* (Ed: I. Piirma), Academic, New York **1982**. b) *Science and Technology of Polymer Colloids Vol. II* (Eds: G. W. Poehlein, R. H. Ottewill, J. W. Goodwin), Martinus Nijhoff, Boston, MA **1983**.

[8] General reviews: a) E. Matijevic, *Acc. Chem. Res.* **1981**, *14*, 22. b) *Fine Particles* (Ed: E. Matijestic), a special issue in *MRS Bull.* **1989**, *14(12)*, 18. c) E. Matijestic, *Chem. Mater.* **1993**, *5*, 412. d) E. Matijevic, *Langmuir* **1994**, *10*, 8.

[9] Reviews on colloidal arrays: a) P. Pieranski, *Contemp. Phys.* **1983**, *24*, 25. b) W. van Megan, I. Snook, *Adv. Colloid Interface Sci.* **1984**, *21*, 119. c) A. P. Gast, W. B. Russel, *Phys. Today* **1998**, *December*, 24. d) *From Dynamics to Devices: Directed Self-Assembly of Colloidal Materials* (Ed: D. G. Grier), a special issue in *MRS Bull.* **1998**, *23(10)*, 21.

[10] J. V. Sanders, *Acta Crystallogr.* **1968**, *A24*, 427.

[11] Two types of crystalline arrays of colloidal spheres (or colloidal arrays) have been extensively studied: the first type includes fcc lattices formed from highly charged colloidal spheres and their volume fractions of colloids are often less than 10 %; the second type is a ccp structure (also a fcc lattice) and its volume fraction of colloids is always close to 74 %. In our discussion, the first type will be referred to as colloidal crystals, and the second type as the so-called synthetic opals, opaline structures, or opaline arrays.

[12] S. Hayashi, Y. Kumamoto, T. Suzuki, T. Hirai, *J. Colloid Interface Sci.* **1991**, *144*, 538.

[13] Y. Xia, J. Tien, D. Qin, G. M. Whitesides, *Langmuir* **1996**, *12*, 4033.

[14] C. Murray, *MRS Bull.* **1998**, *23(10)*, 33.

[15] G. Mie, *Ann. Phys. (Leipzig)* **1908**, *25(4)*, 377.

[16] a) E. M. Zaiser, V. K. LaMer, *J. Colloid Interface Sci.* **1948**, *3*, 571. b) V. K. LaMer, R. H. Dinegar, *J. Am. Chem. Soc.* **1950**, *72*, 4847. c) V. K. LaMer, *Ind. Eng. Chem.* **1952**, *44*, 1270.

[17] W. Stöber, A. Fink, *J. Colloid Interface Sci.* **1968**, *26*, 62.

[18] P. Calvert, *Nature* **1994**, *367*, 119.

[19] M. Ocana, Rodriguez-Clemente, C. J. Serna, *Adv. Mater.* **1995**, *7*, 212.

[20] G. H. Bogush, M. A. Tracy, C. F. Zukoski IV, *J. Non-Cryst. Solids* **1988**, *104*, 95.

[21] M. Ueda, H.-B. Kim, K. Ichimura, *J. Mater. Chem.* **1994**, *4*, 883.

  0935-9648/00/1005-0711 $ 17.50+.50/0

[22] See, for example: a) N. A. M. Verhaegh, A. V. Blaaderen, *Langmuir* **1994**, *10*, 1427. b) S. Y. Chang, L. Liu, S. A. Asher, *J. Am. Chem. Soc.* **1994**, *116*, 6745. c) L. M. Liz-Marzan, M. Giersig, P. Mulvaney, *Langmuir* **1996**, *12*, 4329.
[23] A. J. I. Ward, S. E. Friberg, *MRS Bull.* **1989**, *14(12)*, 41.
[24] J. Ugestad, A. Berge, T. Ellingsen, R. Schmid, T. N. Nilsen, P. C. Mork, P. Stenstad, E. Hornes, O. Olsvik, *Prog. Polym. Sci.* **1982**, *17*, 87.
[25] A. L. Aden, *J. Appl. Phys.* **1951**, *22*, 1242.
[26] Previous work: a) T. Sugimoto, *MRS Bull.* **1989**, *14(12)*, 23. b) M. Ohmori, E. Matijevic, *J. Colloid Interface Sci.* **1992**, *150*, 594. c) W. P. Hsu, R. Yu, E. Matijevic, *J. Colloid Interface Sci.* **1993**, *156*, 56.
[27] Recent studies: a) S. Y. Chang, L. Liu, S. A. Asher, *J. Am. Chem. Soc.* **1994**, *116*, 6739. b) A. P. Philipse, M. P. B. Van Bruggen, C. Pathmamanoharan, *Langmuir* **1994**, *10*, 92. c) D. Walsh, S. Mann, *Nature* **1995**, *377*, 320. d) R. D. Averitt, D. Sarkar, N. J. Halas, *Phys. Rev. Lett.* **1997**, *78*, 4217. e) M. Giersig, L. M. Liz-Marzan, T. Ung, D. Su, P. Mulvaney, *Bunsenges. Phys. Chem.* **1997**, *101*, 1617. f) H. Bamnolker, B. Nitzan, S. Gura, S. Margelo, *J. Mater. Sci. Lett.* **1997**, *16*, 1412. g) S. J. Olderburg, R. D. Averitt, S. L. Westcott, N. J. Halas, *Chem. Phys. Lett.* **1998**, *288*, 243.
[28] *Proc. Mater. Res. Soc.*, Vol. 372 (Eds: D. L. Wilcox, Sr., M. Berg, T. Bernat, D. Kellerman, J. K. Cochran, Jr.), Materials Research Society, Pittsburgh, PA **1994**.
[29] See, for example: H. Huang, E. E. Remsen, T. Kowalewski, K. L. Wooley, *J. Am. Chem. Soc.* **1999**, *121*, 3805.
[30] See, for example: a) A. Garg, E. Matijevic, *J. Colloid Interface Sci.* **1988**, *126*, 243. b) N. Kawahashi, E. Matijevic, *J. Colloid Interface Sci.* **1990**, *138*, 534. c) X. C. Guo, P. Dong, *Langmuir* **1999**, *15*, 5535. d) E. Kumacheva, O. Kalinina, L. Lilge, *Adv. Mater.* **1999**, *11*, 231. e) S. M. Marinakos, J. P. Novak, L. C. Brousseau III, A. B. House, E. M. Ediki, J. C. Feldhaus, D. L. Feldheim, *J. Am. Chem. Soc.* **1999**, *121*, 8518.
[31] a) M. A. Correa-Duarte, M. Giersig, L. M. Liz-Marzan, *Chem. Phys. Lett.* **1998**, *286*, 497. b) T. Ung, L. M. Liz-Marzan, P. Mulvaney, *Langmuir* **1998**, *14*, 3740.
[32] a) F. Caruso, H. Lichtenfeld, M. Giersig, H. Mohwald, *J. Am. Chem. Soc.* **1998**, *120*, 8523. b) F. Caruso, R. A. Caruso, H. Mohwald, *Science* **1998**, *282*, 1111.
[33] Z. Zhong, Y. Yin, B. Gates, Y. Xia, *Adv. Mater.* **2000**, *12*, 206.
[34] See, for example: a) D. G. Gier, *Nature* **1998**, *393*, 621. b) C. A. Murray, *Nature* **1997**, *385*, 203. c) A. E. Larsen, D. G. Grier, *Nature* **1997**, *385*, 230.
[35] a) B. V. Derjaguin, L. Landau, *Acta Physicochim. URSS* **1941**, *14*, 633. b) E. J. W. Verwey, J. T. G. Overbeek, *Theory of the Stability of Lyophobic Colloids*, Elsevier, Amsterdam **1948**. c) J. Visser, in *Surface and Colloid Science*, Vol. 8 (Ed: E. Matijevic), Wiley, New York **1976**, pp. 3–84.
[36] See, for example: a) G. M. Kepler, S. Fraden, *Phys. Rev. Lett.* **1994**, *73*, 356. b) J. C. Crocker, D. G. Grier, *Phys. Rev. Lett.* **1994**, *73*, 352. c) J. C. Crocker, D. G. Grier, *Phys. Rev. Lett.* **1996**, *77*, 1897.
[37] W. R. Bowen, A. O. Sharif, *Nature* **1998**, *393*, 663.
[38] C. A. Murray, D. H. V. Winkle, *Phys. Rev. Lett.* **1987**, *58*, 1200.
[39] A. T. Skjeltorp, P. Meakin, *Nature* **1988**, *335*, 424.
[40] a) N. D. Denkov, O. D. Velev, P. A. Kralchevsky, I. B. Ivanov, H. Yoshimura, K. Nagayama, *Nature* **1993**, *361*, 26. b) G. Picard, *Langmuir* **1998**, *14*, 3710.
[41] a) A. J. Hurd, D. W. Schaefer, *Phys. Rev. Lett.* **1985**, *54*, 1043. b) Z. Horvolgyi, M. Mate, M. Zrinyi, *Colloids Surf. A: Physicochem. Eng. Asp.* **1994**, *84*, 207. c) H. H. Wickman, J. N. Korley, *Nature* **1998**, *393*, 445.
[42] M. Kondo, K. Shinozaki, L. Bergstrom, N. Mizutani, *Langmuir* **1995**, *11*, 394.
[43] a) H. W. Deckman, J. H. Dunsmuir, S. M. Gruner, *J. Vac. Sci. Technol.* **1989**, *B7*, 1832. b) F. Lenzmann, K. Li, A. H. Kitai, H. D. H. Stover, *Chem. Mater.* **1994**, *6*, 156. c) K. U. Fulda, B. Tieke, *Adv. Mater.* **1994**, *6*, 288.
[44] F. Burmeister, C. Schafle, T. Matthes, M. Bohmisch, J. Boneberg, P. Leiderer, *Langmuir* **1997**, *13*, 2983.
[45] See, for example: a) N. D. Denkov, O. D. Velev, P. A. Kralchevsky, I. B. Ivanov, H. Yoshimura, K. Nagayama, *Langmuir* **1992**, *8*, 3183. b) A. S. Dimitrov, K. Nagayama, *Langmuir* **1996**, *12*, 1303. c) O. D. Velev, N. D. Denkov, V. N. Paunov, P. A. Kralchevsky, K. Nagayama, *Langmuir* **1993**, *9*, 3702. d) S. Rakers, L. F. Chi, H. Fuchs, *Langmuir* **1997**, *13*, 7121. e) A. S. Dimitrov, T. Miwa, K. Nagayama, *Langmuir* **1999**, *15*, 5257.
[46] A. S. Dimitrov, C. D. Dushkin, H. Yoshimura, K. Nagayama, *Langmuir* **1994**, *10*, 432.
[47] G. S. Lazarov, N. D. Denkov, O. D. Velev, P. A. Kralchevsky, K. Nagayama, *J. Chem. Soc. Faraday Trans.* **1994**, *90*, 2077.
[48] P. Jiang, J. F. Bertone, K. S. Hwang, V. L. Colvin, *Chem. Mater.* **1999**, *11*, 2132.
[49] H. W. Deckman, J. H. Dunsmuir, S. Garoff, J. A. McHenry, D. G. Peiffer, *J. Vac. Sci. Technol.* **1988**, *B6*, 333.
[50] a) J. C. Hulteen, R. P. V. Duyue, *J. Vac. Sci. Technol.* **1995**, *A13*, 1553. b) J. C. Hulteen, D. A. Treichel, M. T. Smith, M. L. Duval, T. R. Jensen, R. P. V. Duyne, *J. Phys. Chem. B* **1999**, *103*, 3854.
[51] P. Richetti, J. Prost, P. Barois, *J. Phys. Chem.* **1984**, *45*, L1137.
[52] a) M. Trau, D. A. Saville, I. A. Aksay, *Science* **1996**, *272*, 706. b) M. Trau, D. A. Saville, I. A. Aksay, *Langmuir* **1997**, *13*, 6375.
[53] a) S.-R. Yeh, M. Seul, B. I. Shraiman, *Nature* **1997**, *386*, 57. b) Y. Solomentsev, M. Bohmer, J. L. Anderson, *Langmuir* **1997**, *13*, 6058.
[54] M. Giersig, P. Mulvaney, *Langmuir* **1993**, *9*, 3408.
[55] M. Holgado, F. Garcia-Santamaria, A. Blanco, M. Ibsate, A. Cintas, H. Miguez, C. J. Serna, C. Molpeceres, J. Requena, A. Mifsud, F. Meseguer, C. Lopez, *Langmuir* **1999**, *15*, 4701.
[56] See, for example: a) M. M. Burns, J. M. Fournier, J. A. Golovchenko, *Science* **1990**, *249*, 749. b) W. Hu, H. Li, B. Chang, J. Yang, Z. Li, J. Xu, D. Zhang, *Opt. Lett.* **1995**, *20*, 964.
[57] a) H. Misawa, K. Sasaki, M. Koshioka, N. Kitamura, H. Masuhara, *Appl. Phys. Lett.* **1992**, *60*, 310. b) C. Mio, M. D. W. Marr, *Langmuir* **1999**, *15*, 8565.
[58] a) K. E. Davis, W. B. Russel, W. J. Glantschnig, *Science* **1989**, *245*, 507. b) P. N. Pusey, W. van Megen, *Nature* **1986**, *320*, 340.
[59] J. V. Sanders, *Nature* **1964**, *204*, 1151.
[60] a) P. J. Darragh, A. J. Gaskin, J. V. Sanders, *Aust. Gemmol.* **1977**, *November*, 109. b) T. C. Simonton, R. Roy, S. Komarneni, E. Breval, *J. Mater. Res.* **1986**, *1*, 667.
[61] a) A. P. Philipse, *J. Mater. Sci. Lett.* **1989**, *8*, 1371. b) V. N. Bogomolov, S. V. Gaponenko, I. N. Germanenko, A. M. Kapitonov, E. P. Petrov, N. V. Gaponenko, A. V. Prokofiev, A. N. Ponyavina, N. I. Silvanovich, S. M. Samoilovich, *Phys. Rev. E* **1997**, *55*, 7619.
[62] H. Miguez, F. Meseguer, C. Lopez, A. Mifsud, J. S. Moya, L. Vazquez, *Langmuir* **1997**, *13*, 6009.
[63] L. V. Woodcock, *Nature* **1997**, *388*, 235.
[64] A. van Blaaderen, R. Ruel, P. Wiltzius, *Nature* **1997**, *385*, 321.
[65] R. C. Salvarezza, L. Vazquez, H. Miguez, R. Mayoral, C. Lopez, F. Meseguer, *Phys. Rev. Lett.* **1996**, *77*, 4572.
[66] O. Vickreva, O. Kalinina, E. Kumacheva, *Adv. Mater.* **2000**, *12*, 110.
[67] J. Zhu, M. Li, R. Rogers, W. Meyer, R. H. Ottewill, STS-73 Space Shuttle Crew, W. Z. B. Russel, P. M. Chaikin, *Nature* **1997**, *387*, 883.
[68] M. O. Robbins, G. S. Grest, *J. Chem. Phys.* **1988**, *88*, 3286.
[69] Early work: a) N. Ise, *Angew. Chem. Int. Ed. Engl.* **1986**, *25*, 323. b) S. Dosho, N. Ise, K. Ito, S. Iwai, H. Kitano, H. Matsuoka, H. Nakamura, H. Okumura, T. Ono, I. S. Sogami, Y. Ueno, H. Yoshida, T. Yoshiyama, *Langmuir* **1993**, *9*, 394.
[70] Improved methodology: a) N. A. Clark, A. J. Hurd, B. J. Ackerson, *Nature* **1979**, *281*, 57. b) P. Pieranski, L. Strzelecki, B. Pansu, *Phys. Rev. Lett.* **1983**, *50*, 900.
[71] Recent studies: a) T. Okubo, *Langmuir* **1994**, *10*, 1695; *Langmuir* **1994**, *10*, 3529. b) E. A. Kamenetzky, L. G. Magliocco, H. P. Panzer, *Science* **1994**, *263*, 207. c) H. B. Sunkara, J. M. Jethmalani, W. T. Ford, *Chem. Mater.* **1994**, *6*, 362. d) M. Weissman, H. B. Sunkara, A. S. Tse, S. A. Asher, *Science* **1996**, *274*, 959.
[72] See, for example: a) T. B. Mitchell, J. J. Bollinger, D. H. E. Dubin, X. P. Huang, W. M. Itano, R. H. Baughman, *Science* **1998**, *282*, 1290. b) T. M. O'Neil, *Phys. Today* **1999**, *February*, 24.
[73] W. L. Vos, M. Megens, C. M. van Kats, P. Bösecke, *Langmuir* **1997**, *13*, 6004.
[74] T. Okubo, *Langmuir* **1994**, *10*, 1695.
[75] a) D. H. Van Winkle, C. A. Murray, *Phys. Rev.* **1986**, *34*, 562. b) P. Pieranski, L. Strzelecki, B. Pansu, *Phys. Rev. Lett.* **1993**, *50*, 900. c) P. Leiderer, T. Palberg, *Phys. Rev. Lett.* **1997**, *79*, 2348.
[76] a) S. H. Park, D. Qin, Y. X. Xia, *Adv. Mater.* **1998**, *10*, 1028. b) S. Park, Y. Xia, *Langmuir* **1999**, *15*, 266. c) B. Gates, D. Qin, Y. Xia, *Adv. Mater.* **1999**, *11*, 466.
[77] See, for example: a) C. T. Kresge, M. E. Leonowicz, W. J. Roth, J. C. Vartuli, J. S. Beck, *Nature* **1992**, *359*, 710. b) D. D. Archibald, S. Mann, *Nature* **1993**, *364*, 430. c) P. Behrens, G. D. Stucky, *Angew. Chem. Int. Ed. Engl.* **1993**, *32*, 696. d) H. Yang, N. Coombs, G. A. Ozin, *Nature* **1997**, *386*, 692. e) M. Trau, N. Yao, E. Kim, Y. Xia, G. M. Whitesides, I. A. Aksay, *Nature* **1997**, *390*, 674.
[78] a) S. A. Davis, S. L. Burkett, N. H. Mendelson, S. Mann, *Nature* **1997**, *385*, 420. b) A. Imhof, D. J. Pine, *Nature* **1997**, *389*, 948. c) M. Antonietti, B. Berton, C. Goltner, H.-P. Hentze, *Adv. Mater.* **1998**, *10*, 154. d) A. Imhof, D. J. Pine, *Adv. Mater.* **1998**, *10*, 697.
[79] a) O. D. Velev, T. A. Jede, R. F. Lobo, A. M. Lenhoff, *Nature* **1997**, *389*, 447. b) O. D. Velev, T. A. Jede, R. F. Lobo, A. M. Lenhoff, *Chem. Mater.* **1998**, *10*, 3597.

  0935-9648/00/1005-0712 $ 17.50+.50/0

[80] a) S. H. Park, Y. Xia, *Chem. Mater.* **1998**, *10*, 1745. b) S. H. Park, Y. Xia, *Adv. Mater.* **1998**, *10*, 1045. c) B. Gates, Y. Yin, Y. Xia, *Chem. Mater.* **1999**, *11*, 2827.
[81] a) B. T. Holland, C. F. Blanford, A. Stein, *Science* **1998**, *281*, 538. b) B. T. Holland, C. F. Blanford, T. Do, A. Stein, *Chem. Mater.* **1999**, *11*, 795.
[82] S. A. Johnson, P. J. Ollivier, T. E. Mallouk, *Science* **1999**, *283*, 963.
[83] J. S. Yin, Z. L. Wang, *Adv. Mater.* **1999**, *11*, 469.
[84] H. Yan, C. F. Blanford, B. T. Holland, M. Parent, W. H. Smyrl, A. Stein, *Adv. Mater.* **1999**, *11*, 1003.
[85] a) Y. A. Vlasov, N. Yao, D. J. Norris, *Adv. Mater.* **1999**, *11*, 165. b) G. Subramanian, V. N. Manoharan, J. D. Thorne, D. J. Pine, *Adv. Mater.* **1999**, *11*, 1261. c) O. D. Velev, P. M. Tessier, A. M. Lenhoff, E. W. Kaler, *Nature* **1999**, *401*, 548.
[86] a) P. Jiang, J. Cizeron, J. F. Bertone, V. L. Colvin, *J. Am. Chem. Soc.* **1999**, *121*, 7957. b) P. V. Braun, P. Wiltzius, *Nature* **1999**, *402*, 603.
[87] A. A. Zakhidov, R. H. Baughman, Z. Iqbal, C. Cui, I. Khayrullin, S. O. Dantas, J. Marti, V. G. Ralchenko, *Science* **1998**, *282*, 897.
[88] P. Yang, T. Deng, D. Zhao, P. Feng, D. Pine, B. F. Chmelka, G. M. Whitesides, G. D. Stucky, *Science* **1998**, *282*, 2244.
[89] a) J. E. G. J. Wijnhoven, W. L. Vos, *Science* **1998**, *281*, 802. b) M. S. Thijssen, R. Sprik, J. E. G. J. Wijinhoven, M. Megens, T. Narayanan, A. Lagendijk, W. L. Vos, *Phys. Rev. Lett.* **1999**, *83*, 2730.
[90] K. Yoshino, S. B. Lee, S. Tatsuhara, Y. Kawagishi, M. Ozaki, A. A. Zakhidov, *Appl. Phys. Lett.* **1998**, *73*, 3506.
[91] G. Subramania, K. Constant, R. Biswas, M. M. Sigalas, K.-M. Ho, *Appl. Phys. Lett.* **1999**, *74*, 3933.
[92] J. D. Joannopoulos, R. D. Meade, J. N. Winn, *Photonic Crystals*, Princeton University Press, Princeton, NJ **1995**.
[93] E. Yablonovitch, *Phys. Rev. Lett.* **1987**, *58*, 2059.
[94] S. John, *Phys. Rev. Lett.* **1987**, *58*, 2486.
[95] Recent reviews: a) S. John, *Phys. Today* **1991**, *May*, 32. b) E. Yablonovitch, *J. Opt. Soc. Am. B* **1993**, *10*, 283. c) J. D. Joannopoulos, P. R. Villeneuve, S. Fan, *Nature* **1997**, *386*, 143.
[96] Recent special issues: a) *Photonic Band Gap Materials* (Ed: C. M. Soukoulis), Kluwer, Boston, MA **1996**. b) A. Scherer, T. Doll, E. Yablonovitch, H. O. Everitt, J. A. Higgins, a special issue in *J. Lightwave Technol.* **1999**, *17*, 1928.
[97] E. Yablonovitch, T. J. Gmitter, *Phys. Rev. Lett.* **1989**, *63*, 1950.
[98] See, for example: a) K. M. Ho, C. T. Chan, C. M. Soukoulis, *Phys. Rev. Lett.* **1990**, *65*, 3152. b) K. Busch, S. John, *Phys. Rev. E* **1998**, *58*, 3896.
[99] a) C. T. Chan, K. M. Ho, C. M. Soukoulis, *Europhys. Lett.* **1991**, *16*, 563. b) K. M. Ho, C. T. Chan, C. M. Soukoulis, R. Biswas, M. Sigalas, *Solid State Commun.* **1994**, *89*, 413.
[100] L. Isaacs, D. N. Chin, N. Bowden, Y. Xia, G. M. Whitesides, in *Supermolecular Materials and Technologies* (Ed: D. N. Reinhoudt), Wiley, New York **1999**.
[101] a) Y. Fink, A. M. Urbas, M. G. Bawendi, J. D. Joannopoulos, E. L. Thomas, *J. Lightwave Technol.* **1999**, *17*, 1963. b) S. A. Jenekhe, X. L. Chen, *Science* **1999**, *283*, 372. c) J. T. Chen, E. L. Thomas, C. K. Ober, G.-P. Mao, *Science* **1996**, *273*, 343. d) F. S. Bates, G. H. Fredrickson, *Annu. Rev. Mater. Sci.* **1996**, *26*, 501.
[102] A. D. Dinsmore, J. C. Crocker, A. G. Yodh, *Curr. Opin. Colloid Interface Sci.* **1998**, *3*, 5.
[103] a) K. M. Leung, Y. F. Liu, *Phys. Rev. Lett.* **1990**, *65*, 2646. b) Z. Zhang, S. Satpathy, *Phys. Rev. Lett.* **1990**, *65*, 2650. c) H. S. Sozuer, J. W. Haus, R. Inguva, *Phys. Rev. B* **1992**, *45*, 13 962.
[104] A. Moroz, C. Sommers, *J. Phys.: Condens. Matter* **1999**, *11*, 997.
[105] I. I. Tarhan, G. H. Watson, *Phys. Rev. B* **1996**, *54*, 7593.
[106] J. W. Haus, *J. Mod. Opt.* **1994**, *41*, 195.
[107] R. Biswas, M. M. Sigalas, G. Subramania, K.-M. Ho, *Phys. Rev. B* **1998**, *57*, 3701.
[108] a) Z.-Y. Li, J. Wang, B.-Y. Gu, *Phys. Rev. B* **1998**, *58*, 3721. b) Z.-Y. Li, J. Wang, B.-Y. Gu, *J. Phys. Soc. Jpn.* **1998**, *67*, 3288.
[109] M. M. Sigalas, C. M. Soukoulis, R. Biswas, K. M. Ho, *Phys. Rev. B* **1997**, *56*, 959.
[110] K. Busch, S. John, *Phys. Rev. Lett.* **1999**, *83*, 967.
[111] See, for example: a) P. L. Flaugh, S. E. O'Donnell, S. A. Asher, *Appl. Spectrosc.* **1984**, *38*, 847. b) I. M. Krieger, F. M. O'Neill, *J. Am. Chem. Soc.* **1968**, *90*, 3114. c) P. A. Hiltner, I. M. Krieger, *J. Phys. Chem.* **1969**, *73*, 2386. d) J. W. Goodwin, R. H. Ottewill, A. Parentich, *J. Phys. Chem.* **1980**, *84*, 1580.
[112] a) R. J. Spry, D. J. Kosan, *Appl. Spectrosc.* **1986**, *40*, 782. b) P. A. Rundquist, P. Photinos, S. Jagannathan, S. A. Asher, *J. Chem. Phys.* **1989**, *91*, 4932.
[113] W. L. Vos, R. Sprik, A. van Blaaderen, A. Imhof, A. Lagendijk, G. H. Wegdam, *Phys. Rev. B* **1996**, *53*, 16 231.
[114] a) I. I. Tarhan, G. H. Watson, *Phys. Rev. Lett.* **1996**, *76*, 315. b) I. I. Tarhan, M. P. Zinkin, G. H. Watson, *Opt. Lett.* **1995**, *20*, 1571.
[115] W. L. Vos, M. Megens, C. M. van Kats, P. Bosecke, *J. Phys.: Condens. Matter* **1996**, *8*, 9503.
[116] a) R. Mayoral, J. Requena, J. S. Moya, C. Lopez, A. Cintas, H. Miguez, F. Meseguer, L. Vazquez, M. Holgado, A. Blanco, *Adv. Mater.* **1997**, *9*, 257. b) H. Miguez, C. Lopez, F. Mesequer, A. Blanco, L. Vazquez, R. Mayoral, M. Ocana, V. Fornes, A. Mifsud, *Appl. Phys. Lett.* **1997**, *71*, 1148. c) C. Lopez, L. Vazquez, F. Meseguer, R. Mayoral, M. Ocana, H. Miguez, *Superlattices Microstruct.* **1997**, *22*, 399.
[117] a) V. N. Astratov, Y. A. Vlasov, O. Z. Karimov, A. A. Kaplyanskii, Y. G. Musikhin, N. A. Bert, V. N. Bogomolov, A. V. Prokofiev, *Phys. Lett. A* **1996**, *222*, 349. b) Y. A. Vlasov, V. N. Astratov, O. Z. Karimov, A. A. Kaplyanskii, V. N. Bogomolov, A. V. Prokofiev, *Phys. Rev. B* **1997**, *55*, R 13 357.
[118] D. Mei, H. Liu, B. Cheng, Z. Li, D. Zhang, *Phys. Rev. B* **1998**, *58*, 35.
[119] J. F. Bertone, P. Jiang, K. S. Hwang, D. M. Mittleman, V. L. Colvin, *Phys. Rev. Lett.* **1999**, *83*, 300.
[120] Y. A. Vlasov, K. Luterova, I. Pelant, B. Honerlage, V. N. Astratov, *Appl. Phys. Lett.* **1997**, *71*, 1616.
[121] a) B. Gates, S. H. Park, Y. Xia, *J. Lightwave Technol.* **1999**, *17*, 1956. b) B. Gates, Y. Xia, unpublished.
[122] H. Miguez, F. Meseguer, C. Lopez, A. Blanco, J. S. Moya, J. Requena, A. Mifsud, V. Fornes, *Adv. Mater.* **1998**, *10*, 480.
[123] B. Bates, S. H. Park, Y. Xia, *Adv. Mater.* **2000**, *12*, 653.
[124] See, for example: a) S. Fan, P. R. Villeneuve, R. D. Meade, J. D. Joannopoulos, *Appl. Phys. Lett.* **1994**, *65*, 1466. b) C. C. Cheng, A. Scherer, *J. Vac. Sci. Technol. B* **1995**, *13*, 2696. c) S. Noda, N. Yamamoto, A. Sasaki, *Jpn. J. Appl. Phys.* **1996**, *35*, L909. d) J. S. Foresi, P. R. Villeneuve, J. Ferrera, E. R. Thoen, G. Steinmeyer, S. Fan, J. D. Joannopoulos, L. C. Kimerling, H. I. Smith, E. P. Ippen, *Nature* **1997**, *390*, 143. e) S. Y. Lin, J. G. Fleming, D. L. Hetherington, B. K. Smith, R. Biswas, K. M. Ho, M. M. Sigalas, W. Zubrzycki, S. R. Kurtz, J. Bur, *Nature* **1998**, *394*, 251.
[125] L. I. Berger, *Semiconductor Materials*, CRC Press, Boca Raton, FL **1997**.
[126] See, for example: C. A. Murray, D. G. Grier, *Am. Sci.* **1995**, *83*, 238.
[127] See, for example: P. Calvert, *Nature* **1985**, *317*, 201.
[128] H. W. Deckman, J. H. Dunsmuir, *Appl. Phys. Lett.* **1982**, *41*, 377.
[129] C. B. Roxlo, H. W. Deckman, B. Abeles, *Phys. Rev. Lett.* **1986**, *57*, 2462.
[130] Y. C. Fisher, H. P. Zingsheim, *J. Vac. Sci. Technol.* **1981**, *19*, 881.
[131] H. W. Deckman, T. D. Moustakas, *J. Vac. Sci. Technol. B* **1988**, *6*, 316.
[132] C. B. Roxlo, H. W. Deckman, J. Gland, S. D. Cameron, R. R. Chianelli, *Science* **1987**, *235*, 1629.
[133] M. C. Buncick, R. J. Warmack, T. L. Ferrell, *J. Opt. Soc. Am. B* **1987**, *4*, 927.
[134] a) H. Fang, R. Zeller, P. J. Stiles, *Appl. Phys. Lett.* **1989**, *55*, 1433. b) M. Green, M. Garcia-Parajo, F. Khaleque, *Appl. Phys. Lett.* **1993**, *62*, 264.
[135] W. D. Dozier, K. P. Daly, R. Hu, C. E. Platt, M. S. Wire, *IEEE Trans. Magn.* **1991**, *27*, 3223.
[136] a) J. Boneberg, F. Burmeister, C. Schafle, P. Leiderer, D. Reim, A. Fery, S. Herminghaus, *Langmuir* **1997**, *13*, 7080. b) F. Burmeister, C. Schafle, B. Keilhofer, C. Bechinger, J. Boneberg, P. Leiderer, *Adv. Mater.* **1998**, *10*, 495.
[137] R. Wiesendanger, M. Bode, M. Kleiber, M. Lohndorf, R. Pascal, A. Wadas, D. Weiss, *J. Vac. Sci. Technol. B* **1997**, *15*, 1330.
[138] a) K. Douglas, N. A. Clark, *Appl. Phys. Lett.* **1990**, *56*, 692. b) K. Douglas, G. Devaud, N. A. Clark, *Science* **1992**, *257*, 642.
[139] a) J. M. Weissman, H. B. Sunkara, A. S. Tse, S. A. Asher, *Science* **1996**, *274*, 959. b) G. Pan, R. Kesavamoorthy, S. A. Asher, *Phys. Rev. Lett.* **1997**, *78*, 3860. c) G. Pan, R. Kesavamoorthy, S. A. Asher, *J. Am. Chem. Soc.* **1998**, *120*, 6525.
[140] a) J. H. Holtz, S. A. Asher, *Nature* **1997**, *389*, 829. b) J. H. Holtz, J. W. Holtz, C. H. Munro, S. A. Asher, *Anal. Chem.* **1998**, *70*, 780.
[141] See, for example: R. Dagani, *Chem. Eng. News* **1997**, *June 9*, 26.
[142] a) S. Hachisu, S. Yoshimura, *Nature* **1980**, *283*, 188. b) P. Bartlett, R. H. Ottewill, P. N. Pusey, *Phys. Rev. Lett.* **1992**, *68*, 3801.
[143] T. Sugimoto, M. M. Khan, A. Muramatsu, *Colloids Surf. A* **1993**, *70*, 167.
[144] A. T. Skjeltorp, J. Ugelstad, T. Ellingsen, *J. Colloid Interface Sci.* **1986**, *113*, 577.
[145] H. R. Sheu, M. S. El-Aasser, J. W. Vanderhoff, *Polym. Mater. Sci. Eng.* **1987**, *57*, 911.
[146] Y. Lu, Y. Yin, Y. Xia, unpublished result.
[147] M. Nagy, A. Keller, *Polym. Commun.* **1989**, *30*, 130.
[148] K. M. Keville, E. I. Franses, J. M. Caruthers, *J. Colloid Interface Sci.* **1991**, *144*, 103.

  0935-9648/00/1005-0713 $ 17.50+.50/0